# Lynx1 and the β2V287L Mutation Affect the Stoichiometry of the α4β2 Nicotinic Acetylcholine Receptor

Thesis by

**Weston A. Nichols**

In Partial Fulfillment of the Requirements for the Degree of

Doctor of Philosophy


California Institute of Technology
Pasadena, California

2014

(Defended May 1, 2014)

*To my mother, father, and Peden.*

Acknowledgements

First and foremost, thank you to Henry Lester, my Ph.D. advisor. Henry accepted me into his lab before it was clear that I would be useful as a graduate student, and provided me with a wonderfully appropriate mix of guidance and freedom. Early on, I wanted to start as many projects as possible, and pitched many that made no sense from a practical perspective, and probably several other perspectives. Henry told me not to do them in a way that forced me to learn the process of scientific diligence, and to take ownership of the projects I did pursue. Henry taught me this process by spending a lot of time with me through many meetings, including Fluorescence Club, α Club, and going for coffee at the Red Door. One of the most salient items that Henry taught me is how to plod through data slowly to come to a deeper understanding of the data and how (or if) it fits into a larger picture. I think this is something that is very hard to teach. Henry did it by spending a lot of time with me.

Thank you to my thesis committee, Ray Deshaies, Dennis Dougherty, and David Prober. You have been great to me, and provided much helpful advice.

Thank you to everyone in the Lester Lab during my time here. Thank you to Eloisa Imel for welcoming me to the lab when I was starting and helping with many issues along the way. Thanks to Purnima for ordering and equipment maintenance, which allowed me to always keep experiments going. Thanks to Elisha Mackey for teaching me how to clone efficiently when I first started in the Lester Lab. Thanks to the other grad students, Crystal Dilworth, Rell Parker, and Teagan Wall for many great discussions, help with experiments, and camaraderie. Thanks to many former members of the lab who taught me much about science, trained me in a wide array of experimental techniques and helped me troubleshoot: Beverly Henley, Rachel Penton, Ying Wang, Cheng Xiao, Charlene Kim, and Jonathan Wang.

Thank you to Chris Richards for teaching me the process of science at a high level and how to implement experiments at a technical level. Thank you also for bringing me up to speed very quickly on microscopy and neuronal culture when I was a new hire and you were focused on becoming a professor. Thanks to Chris and Rahul Srinivasan for teaching me the majority of what I know about microscopy. Thanks to Brandon Henderson for teaching me a great deal about pharmacology and chemistry, and for performing the electrophysiology experiments on mammalian cells in this thesis.

Thank you to Shawna Frazier for many things including teaching me how to use the FlexStation and the finer points of dose-response relations. More importantly, thank you for your companionship and causing me to look forward to weekends in lab. Perhaps now is an appropriate time to reveal… that I did not read the manual.

Thank you to Bruce Cohen for sharing his vast knowledge of electrophysiology, neuroscience and ADNFLE, and for fun and educational discussions on a wide range of topics including pharmacology, ADNFLE, finance and real estate, cooking, meditation, and many more.

Thank you to Julie Miwa (who discovered lynx1) for getting me started in the Lester Lab, and for guidance and leadership on the lynx portion of this thesis.

Thank you to Caroline Yu for her extremely competent and diligent help with both executing and planning experiments relevant to both the lynx and β2VL sections of this thesis. I am incredibly lucky to have worked with Caroline, an undergrad with incredible work ethic, excellent training from prior work with Chris Richards and Henry Lester, and the ability to quickly learn new concepts and techniques. I hope I can work with Caroline again someday.

Thank you to the members of the Dougherty Lab, and especially to Chris Marotta for collaborating with me on the β2VL paper, and to Tim Miles for a great deal of technical help to Caroline and me with imaging experiments.

Thank you to Bruce Hay, especially for support before I joined Henry's lab. Our meetings during that time meant a great deal to me. Thank you for remaining committed.

Thank you to Liz Ayala for making the administrative tasks easy for me, and for knowing and sharing how to get things done.

Thank you to all my friends in Biology, and especially Mike Rome, Alex Webster, Eric Erkenbrack, and Jon Valencia.

Thank you to Samy Hamdouche, my roommate and great friend. Together, we have set and achieved goals in a wide variety of different fields in the four years we have known each other. The coming years are going to be fun.

Finally, thank you to my family: Mom, Dad, and Peden; I love you big time.

Table of Contents

# Chapter I:
# Introduction

In his studies of the neuromuscular junction in 1851, Claude Bernard discovered that signals could be transmitted between cells by chemicals that we now call neurotransmitters. He demonstrated that curare, a toxin isolated from plants used to make arrow toxins for hunting, could block this transmission in a reversible manner. Today, we know that curare acts as a competitive antagonist to acetylcholine blocking neurotransmission at the nerve-muscle junction and causing paralysis. Nicotine binds and activates several of these receptor types, which are therefore called the nicotinic acetylcholine receptors (nAChRs). Over the past 25 years, a great deal of progress has been made towards understanding both the molecular and biophysical properties of nAChRs, as well as their relevance towards important biological processes in the brain.

***The nicotinic acetylcholine receptors***

The nAChRs are pentameric, ligand-gated ion channels. Their endogenous ligand, acetylcholine, as well as pharmacological agents such as nicotine, activate the channels. The specific proteins that make up the receptors for acetylcholine have been identified, cloned, and several can be expressed in heterologous systems such as *Xenopus laevis* oocytes or human embryonic kidney (HEK) cells. Heterologous expression enables the use of electrophysiology and microscopy to conduct precise pharmacological and biophysical experiments, several of which are described in this thesis.

Neuronal nAChRs are expressed throughout the central and peripheral nervous system, and are made up of nine different α subunits and three different β subunits in both heteropentameric and homopentameric combinations such as α4β2 and α7, respectively. Different subtypes have sensitivities to ACh that vary over 3-4 orders of magnitude. The

most widely expressed receptor, α4β2, has two stoichiometries: $(\alpha4)_2(\beta2)_3$ and $(\alpha4)_3(\beta2)_2$, with ACh sensitivities of approximately 1 μM and 80 μM, respectively. Gating of the channel results in permeability to $Na^+$, $K^+$, and, for some receptor subtypes, $Ca^{2+}$. In general, activation of nAChRs in the brain regulates the amount of other neurotrasmitters realeased into synaptic clefts, including dopamine, serotonin, GABA, and glutamate. Thus, nAChRs can be thought of as commonly functioning as performing a tuning function, or "volume knob" for other neurotransmitter systems.

Most nAChRs in the brain are expressed at presynaptic terminals (Gotti et al., 2006), where they are able to modulate neurotransmitter release. ACh is released into the synaptic cleft and then rapidly degraded by GPI-anchored acetylcholinesterase (AChE) enzymes. While ACh is present, it binds to nAChRs causing activation and gating, but prolonged exposure results in desensitization, a closed channel state with ACh (or another ligand) bound, that is more stable than the open channel conformation.

Nicotinic receptors are also found on the somatodendritic areas of the plasma membrane, which led to the volume transmission hypothesis that ACh that has escaped degradation within the synaptic cleft can diffuse out toward neuronal cell bodies, binding and activating receptors there. For this to happen, enough ACh would have to escape degradation, and likely more sensitive receptors would have to be expressed on the somatodendritic compartment. Another effect of somatodendritic localization of receptors could be activation by other endogenous ligands that are not degraded rapidly, namely choline, which activates α7.

***The molecular structure of nAChRs***

Unwin and colleagues performed electron microscopic reconstruction, at increasing resolution, of the muscle-type nAChR receptor over ~3 decades, using samples derived from the postsynaptic membranes of the *Torpedo* ray electric organ (Miyazawa et al., 2003; Unwin, 2005). The *Torpedo* electric organ has been a useful model system due to its high concentration of ACh receptors and relative ease of isolation from the animal. The papers in 2003 and 2005 revealed a barrel-structured cylinder with a diameter of ~8 nm and length of ~16 nm, organized as a pentamer of subunits arranged around a central pore, that can be divided into extracellular (ECD), transmembrane (TMD), and intracellular (ICD) domains. The TMD is composed of 4 membrane-spanning α-helices, with the second (TM2) arranged so that it lines the water-filled pore of the channel. TM1, 3, and 4 lie outside the pore, and contact the membrane, providing an opportunity for the lipid composition of local membrane to interact with and possibly influence the gating properties of the channel.

Within the membrane, the pore-lining TM domains have open and closed configurations or differing levels of stability. These biophysical properties of the pore region determine the activation and desensitization kinetics of the channel, which vary widely across nAChR subtypes. When the channel is closed, the TM2 helices are shifted inward, blocking the passage of ions across the membrane. Upon activation by a ligand, the TM2 helices shift away from the center, allowing ions to pass through. However, the closed state is more stable than the open state when ligand is bound, which leads to a desensitized state with ligand bound and the channel closed. Most ligand-gated ion channels likely share this allosteric mechanism.

The cytoplasmic domain or ICD of nAChRs consists mostly of a connecting loop between the TM3 and TM4 domains. This loop varies greatly between subunits both is sequence and in length. The cytoplasmic loop has several functions that govern properties of the channel. The muscle subunits have several phosphorylation sites that control receptor desensitization (Swope et al., 1995), and the β2 subunit interacts with several cytoskeletal proteins including dynamin, tubulin, and clathrin, in addition to interacting with GPCR systems (Kabbani, 2008). Targeting the intracellular domain might be fruitful for drug discovery due to the diversity between subunits, and thus opportunity to achieve selectivity between them. To do this successfully, much more work is needed to determine how modifications to the intracellular loops might impact both the biophysics of the channel and the consequences on the downstream biology.

The crystal structure of the snail, *Lymnaea stagnalis,* acetylcholine-binding protein (AChBP) was solved in 2001, and provided a basis for the structure of the ligand-binding ECD of the nAChR (Hansen et al., 2006). AChBP is a soluble pentamer that binds up to 5 ACh molecules at the interfaces between subunits. In support of the use of AChBP as a model for the ECD, it also binds to nicotine, curare, and α-bungarotoxin, and is likely most closely related to the α subunits of the nAChRs (Hansen et al., 2006), and has been used widely as a tool for screening of drug candidates targeting nicotinic receptors. Each subunit folds into a β-sheet sandwich composed of 6 inner sheets and 4 outer sheets. The ECD confers the differential selectivity of ligands. A deeper understanding of how ligands interact with the ECD at both the orthosteric sites (competitive with ACh) and allosteric sites (non-competitive with ACh) is required to design ligands and drugs that selectively target some nAChR subtypes over others.

### *The biological importance of nAChRs*

The cholinergic system is important in a wide variety of neuronal and cognitive processes, including addiction and reward (Tang and Dani, 2009), cognition (Levin, 2002), mood (Picciotto et al., 2008), pain (Decker et al., 2001), and possibly neuroprotection from disease (Hernan et al., 2002). Here, I provide a brief review of some of the current controversies relating to the applicability of nAChR biology to these processes.

### *Addiction and reward*

While approximately 40% of smokers attempt to quit in a given year, only 10% of those who attempt will successfully abstain for a full year (Gonzales et al., 2006). Smoking is a leading cause of preventable death, and pharmacotherapies to increase quitting success rates would be highly valuable for public health. An enormous amount of progress has been made over the past decade in elucidating the specific brain regions and receptors responsible for nicotine addiction. This led to the rational design and FDA approval of varenicline, a novel drug for smoking cessation. Although quitting success rates for patients taking varenicline were double those for placebo, the overall quit rate was modest at around 9% across many studies (Cahill et al., 2013).

Nicotine induces long-term potentiation (LTP) in a dose-dependent manner through increased dopamine release in the ventral tegmental area (VTA) (Mansvelder and McGehee, 2000). This process is likely the underlying mechanism for nicotine's ability to both cause pleasure in the mesolimbic dopamine "pleasure" circuitry, and also to induce long lasting changes in connections between neurons that comprise the learning process of

becoming addicted. This mechanism is likely a general one that may apply to all addictive drugs, and even other addictions such as food and other behavioral addictions. Indeed, activation of dopaminergic neurons in the VTA occurs with all well-studied drugs of abuse (Leslie et al., 2013).

Two predominant pharmacological strategies for treatment of nicotine addiction to decrease the rate of patients returning to smoking have emerged. The first is to decrease signaling through β2* nAChRs in the VTA. This strategy is supported by experiments done using knock-out mice and by the clinical success, although modest, of varenicline. The second strategy is to increase signaling through α5* nAChRs in the MHb, which mediate the aversive reaction to higher doses of nicotine.

Several types of nAChR subunits are expressed in the VTA, including β2, α4, and α6. Knock-out (KO) mice have been made for each of these subunits, and the knocked-out subunits can be selectively re-expressed in specific brain regions. Nicotine self-administration experiments have shown that β2-KO, α4-KO, and α6-KO mice do not respond to nicotine, but that selective re-expression in the VTA of the knocked out subunit regain nicotine self-administration behavior (Pons et al., 2008). These experiments provide excellent evidence that all three subunits may be required in the VTA for nicotine addiction, and suggest that pharmacological inhibition of the signal through these receptors could be useful as a smoking cessation aid.

Three distinct classes of drugs could be utilized to achieve this outcome: antagonists that selectively block channel opening, partial agonists that activate the channel with lower efficacy than endogenous ACh or nicotine, of negative allosteric modulators (NAMs) that lower the efficacy or increase the potency of ACh/nicotine. The most favored

strategy is to use a partial agonist because they may work via two distinct mechanisms. First, they activate the channel at a lower level than endogenous ACh or nicotine, but may cause enough dopamine release to mitigate the sensations of craving and withdrawal. Second, partial agonists may reduce the acute positive sensations of smoking nicotine by acting as an antagonist when other agonists with greater efficacy (nicotine) are present. Varenicline is a weak partial agonist on α4β2, with a relative efficacy of <15% compared to nicotine or ACh, Antagonists or NAMs would theoretically achieve the second mechanism of decreasing the reward received from nicotine administration, but would not replicate the low-level dopamine release of partial agonists, and therefore are less likely to reduce craving and withdrawal symptoms.

While a partial agonist strategy on α4β2 or α6α4β2 in the VTA appears to be promising for nicotine addiction, and varenicline, an α4β2 partial agonist with ~13% efficacy compared to ACh, has been tested extensively in humans and even approved by the FDA, its efficacy is modest, with less than ten percent of patients abstaining from smoking for one year. Varenicline may also be a partial agonist on α6α4β2, but we have less certainty because of challenges regarding functional expression of α6* nAChRs.

The second strategy is to increase signal from α5* nAChRs in the medial habenula (MHb), which mediate the aversive stimulus of higher doses of nicotine. The α5D398N variant is associated with higher rates of nicotine addiction in humans, and inclusion of the 398N variant exhibits reduced receptor function in vitro (Bierut et al., 2008). Experiments in α5-KO mice have demonstrated that removal of α5 results in the loss of aversion to high doses of nicotine (Fowler et al., 2011). Additionally, re-expression of α5 in the MHb restores aversion to nicotine.

Taken together, these experiments provide a strong rationale for the development of an α5 positive allosteric modulator (PAM) to increase the aversive stimulus received from nicotine. A similar aversion therapy strategy is currently employed to treat severe alcohol abuse using the drug Antabuse (disulfuram) as conditional emetic. Disulfiram produces an acute emetic response when combined with alcohol, creating a strong deterrent to consumption, especially after the effects are experienced once. One major limitation is that patients realize that the drug is causing the emetic effects, and therefore plan to stop taking the drug and resume alcohol consumption. Frequently, patients are placed on a program whereby another person must watch the addict take the pill each day, with visual confirmation that the pill has been swallowed. Although burdensome, a similar method could be implemented with patients addicted to nicotine.

***Cognition and schizophrenia***

The symptoms of schizophrenia can be divided into three categories: positive, negative, and cognitive. The positive symptoms are psychotic in nature, consisting of hallucinations and delusions. The negative symptoms are primarily flat affect, anhedonia, and depression, while the cognitive symptoms involve deficits in working memory, attention, and executive functioning. The negative and cognitive symptoms often precede positive symptom onset (Addington and Addington, 1993), and persist even after the positive symptoms have been treated successfully by commonly used antipsychotics, which alleviate positive symptoms in the majority of patients(Erhart et al., 2006).

All clinically effective antipsychotics used to treat the positive symptoms of schizophrenia have diverse and complex polypharmacology; each individual drug has

activity on a wide range of targets in the CNS (Roth et al., 2004). One commonality between these drugs is that they all act as either an antagonist or a partial agonist on the dopamine D2 receptor. This common mechanism is widely accepted as the mechanism by which they exert their effect on the positive symptoms of schizophrenia(Seeman, 2002).

While effective therapies may light the way for development of better treatment of positive symptoms, that luxury does not exist for the negative and cognitive symptoms of schizophrenia. The α7 nAChR has become a widely investigated target for treatment of the cognitive and negative domains due to evidence from both in vivo experiments and human clinical data. Initially, it was found that α7 antagonists could induce sensory gating deficits in auditory evoked potential responses (Luntz-Leybman et al., 1992), consistent with similar gating deficits in schizophrenics, and later in genetic mouse models of schizophrenia (Lipska and Weinberger, 2000). Additionally, post-mortem studies of human brains revealed a los of α7 nAChRs in schizophrenic patients (Freedman et al., 1995), supporting a hypothesis that increasing signal through α7 may restore a pre-existing deficit in schizophrenics.

Interpretation of auditory gating experiments is complicated by the fact that some non-schizophrenic patients (2-5% of the population) display deficits in gating but no symptoms of schizophrenia. Interestingly, several drugs, including nicotine, have demonstrated the ability to normalize sensory gating abnormalities, but have not had a large effect on clinically detectable endpoints associated with measures of negative or cognitive symptoms. However, an overwhelming majority of schizophrenics smoke (>90%), and they tend to extract more nicotine per puff than normal patients (Williams et al., 2005), which is viewed as evidence of self-medication with nicotine.

Several agonists an partial agonists have been tested recently in clinical trials, and although some rescued sensory gating and showed initial signs of improvement in the form of increased attention and working memory (Gault et al., 2013; Lieberman et al., 2013), the results were judged to not warrant further development for both TC-5619 and ABT-126.

Another compound, EVP-6124 may act by potentiating the endogenous response of α7 to ACh, as opposed to activating or desensitizing the channel. Interestingly, EVP-6124 appears to potentiate the receptor at a concentration of 2 nM, which is below concentrations required for appreciable activation (Prickaerts et al., 2012). If this mechanism is responsible for the pro-cognitive effects seen in early-stage clinical trials, PAMs may provide an attractive modality to achieve a stronger therapeutic effect while reducing the confounding effects of activation and/or desensitization.

Thus far, PAMs have not been investigated thoroughly due to possible toxicities associated with type II PAMs, and the lack of available molecules that act as type I PAMs. PAMs are defined by their ability to increase current magnitude, receptor sensitivity, and Hill coefficients by binding at an allosteric site on the receptor. Type I PAMs achieve this with little or no effect on the response waveform in terms of channel open time or desensitization kinetics. Type II PAMs, on the other hand, do slow desensitization kinetics, and may cause desensitized to channels to return to an active state as well, while ligand is bound (Williams et al., 2011).

Two major concerns with type II PAMs predominate. First, the alteration of the response waveform, and thus the kinetics of calcium influx into the cell, may change the quality of information transmitted to the receiving cell, and the downstream signaling milieu. Second, large increases in intracellular calcium are associated with excitotoxicity

and cell death (Williams et al., 2012). Although some studies have found that type II PAMs can be used effectively on rat neurons in vitro without excitoxicity (Hu et al., 2009), rat neurons may be heartier than those from a mouse or human, and toxicity concerns will predominate when moving into the clinic in elderly Alzheimer's patients whose neurons may be more vulnerable to increased intracellular calcium.

For the reasons above, type I PAMs may be an attractive way of testing the hypothesis that increasing signal through α7 could be therapeutically valuable. Type I PAMs have been challenging to create from a medicinal chemistry perspective because most HTS technologies are unable to detect them due to the rapid desensitization kinetics of α7. Recently, several type II PAMs have been found, and a couple are in the process of entering the clinic (Pandya and Yakel, 2013). Some of these compounds may also have activity on other receptors, such as GABA or 5HT3, so a pure interpretation of their actions on α7 leading to improvements in cognitive function may not be possible.

***Mood***

Individuals with major depressive disorder (MDD) have higher rates of nicotine dependence (50-60%) than the general population (25%) (Glassman et al., 1990). Furthermore, in MDD patients, quitting smoking can exacerbate depressive symptoms leading to serious major depression. Other clinical studies have demonstrated an anti-depressant effect of nicotine patches in non-smoker MDD patients (SalÃn-Pascual et al., 1996), and at least two marketed anti-depressants have demonstrated efficacy for smoking cessation: buproprion (Hurt et al., 1997) and nortriptyline (Hall et al., 1998). Because nicotine, and all known nAChR agonists cause both activation and desensitization of the

receptor, it is difficult to separate the two in order to attribute any observed effect to one of the other. Chronic nicotine also upregulates the amount of nAChRs on the plasma membrane (Buisson and Bertrand, 2001), further complicating interpretation of longer term use.

The Flinders Sensitive Line (FSL) of rats provided strong support for the hypothesis that increased cholinergic tone can be involved in mood disorders, including depression (Mineur et al., 2011). FSL rats were bred for increased sensitivity to an acetylcholinesterase drug, diisopropylfluorophosphonate (DFP), resulting in abnormally high levels of ACh, and chronically increased cholinergic tone when exposed to the drug (Overstreet and Russell, 1982). FSL rats display several behavioral phenotypes associated with depression including increased anhedonia (Pucilowski et al., 1993), and reduced locomotor activity, weight and REM sleep (Overstreet, 1993). Furthermore, chronic stress (induced via inescapable foot shock plates or swim stress tests) can also induce supersensitivity of the cholinergic system in rats (Dilsaver et al., 1986). Taken together, the preclinical rational for increased cholinergic tone playing a role in depressive behavior is strong.

If desensitization, and reduction of signal through nAChRs, is the mechanism by which nicotinic agonists could exert an anti-depressant effect, then we might expect an antagonist to reproduce the effect. The S-(+)-enantiomer of mecamylamine (TC-5214) was developed for the treatment of MDD (Rabenstein et al., 2006), and although results were promising both pre-clinically (Lippiello et al., 2008), and in an early phase 2 trial (Dunbar, 2010), they were not successfully repeated and development has been discontinued, casting

doubt on the hypothesis that the reduced signal aspect of desensitization is the sole mechanism whereby cholinergic ligands might treat depression.

***nAChR agonists for analgesia***

Since the 1930's we have known that nicotine acts as relatively weak analgesic, but little attention was paid to development of nAChR agonists as pain therapeutics until the discovery of epibatidine in 1976 by John Daly. Epibatidine is a potent nAChR agonist, with structural similarities to nicotine (Fig 1-1), isolated from the skin of the Ecuadorean poisonous dart frog species *Epipedobates tricolor*. Several factors prevented researchers from obtaining large enough amounts of the drug to perform experiments, including the endangered status of the animal, its inability to synthesize the molecule in captivity (on its own without consuming it from prey), and the lack of analytical tools to identify the specific compound from the frog's skin that produced the effect.

Eventually, the invention of nuclear magnetic resonance (NMR) spectroscopy enabled the discovery of the structure of epibatidine (Spande et al., 1992), leading to synthetic production of the compound in large quantities (Corey et al., 1993).

Epibatidine's use as a drug is limited by significant on-target toxicity with a small therapeutic window; the efficacious dose is very close to a lethal one. However, because epibatidine acts as a broad agonist on many nAChR subtypes, the possibility for more selective agonism was promising for a potential analgesic. Several nAChR agonists were developed that demonstrated improved safety profiles with retained anti-nociceptive activity in preclinical models. One such ligand, ABT-594, demonstrated similar potency on $\alpha4\beta2$, but >1,000 fold less activity on muscular ACh receptors (Kesingland et al., 2000),

was developed through phase 2 trials, but discontinued due to gastrointestinal side effects, and possibly others. Nicotinic agonists have demonstrated efficacy at analgesia, and remain promising targets due to potential advantages over opioids through greater efficacy by more potent inhibition of pain and lack of tolerance, and lack of common opioid-related side effects including respiratory depression, cognitive impairment, dependency, and withdrawal. Thus far, separating the desirable anti-nociceptive effects from intolerable side effects has proven elusive.

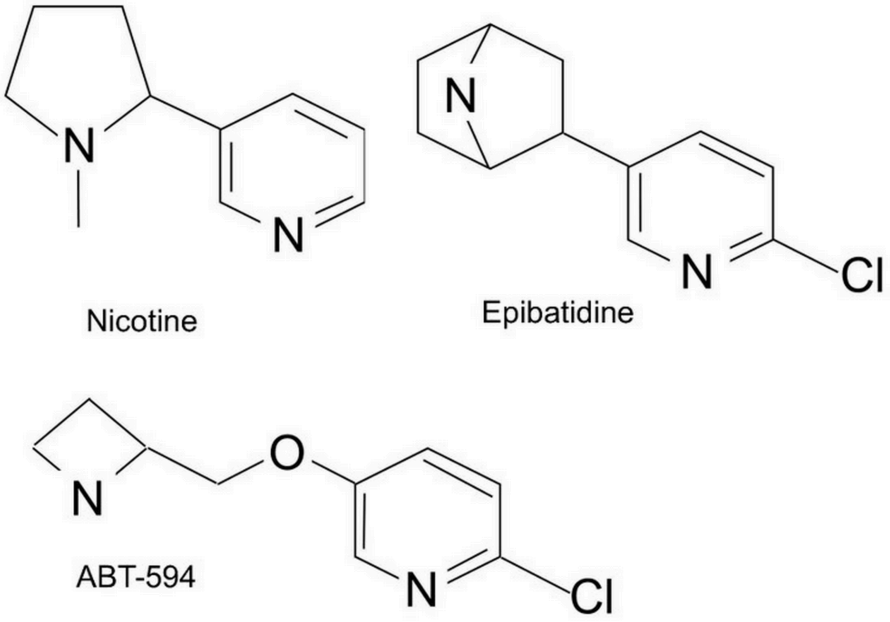


Figure 1-1. Structures of nicotine, epibatidine, and ABT-594.

***Nicotine and neuroprotection from disease***

Nicotine usage by smoking cigarettes may exert neuroprotective effects against developing Parkinson's disease (PD) and Alzheimer's disease. Thus far, the evidence is stronger for PD protection. Data from retrospective epidemiological studies demonstrates that compared to never smokers, smokers have a lower risk of developing PD by a factor of

0.39 (a 61% reduction in risk) for current smokers, and 0.80 for past smokers (Hernan et al., 2002). A similar retrospective analysis conducted on pairs of twins, wherein at least one twin had PD, demonstrated that those without PD tended to smoke an average of 9.8 pack years more than the PD twin ($p=0.026$) (Tanner et al., 2002). The design of this twin study makes it unlikely that either genetic or environmental factors confound the signal of lower risk of PD among smoker.

One competing hypothesis is that early, undetected PD onset may cause a patient to quit smoking, perhaps by making it less rewarding due to disruption of the midbrain dopaminergic system. However, similar associations were found when smoking dosage was calculated only until 10 years before clinical onset of PD, suggesting that undetected PD onset is less likely to cause a patient to stop smoking, thus accounting for the association. These results are consistent with an interpretation that smoking exerts a neuroprotective effect on PD, but an early prodromal effect diminishing smoking behavior cannot be ruled out definitively. Furthermore, although evidence for the neuroprotective effect of smoking is substantial, more experiments are necessary to determine if nicotine alone, as opposed to smoking, can exert a similar effect.

***Drugs targeting nAChRs***

Although pharmacological targeting of nAChRs holds promise for a wide range of conditions, the FDA has approved few drugs targeting this mechanism. Nicotine itself is approved for smoking cessation as nicotine replacement therapy. Varenicline is also approved for smoking cessation. Cytisine is approved for the same indication in some European countries. Mecamylamine, an nAChR antagonist, was approved and marketed in

the 1950s for hypertension, but was discontinued due to side effects resulting from non-specific blockage of nAChRs in the ganglionic system, causing inhibition of both the sympathetic and parasympathetic nervous system. Finally, buproprion is also approved for smoking cessation, but in addition to acting as an antagonist on nAChRs, inhibits the dopamine and norepinephrine transporters.

The diversity of nAChRs subtypes and differential expression in different brain regions provides a plausible rationale by which a pharmacological agent could achieve specificity and perhaps treat a condition with few side effects. A deeper understanding of the composition of the various subtypes, where they are expressed both on the plasma membrane of the cell and in which neuronal subtypes, and how the biophysical structures interact with specific ligands is critical to design therapeutics targeting the neuronal cholinergic system.

The nAChR subtype studied in this thesis is α4β2, which is the most abundant receptor in the human brain. Experiments on heterologously expressed receptors in oocytes demonstrated that varying the ratio of α4:β2 RNA injected into the oocyte could change the electrophysiological properties of the resulting receptors (Zwart and Vijverberg, 1998). This is due to the presence of two stoichiometries: a lower sensitivity $(\alpha4)_3(\beta2)_2$, and a higher sensitivity $(\alpha4)_3(\beta2)_2$ receptor (Fig 1-2).

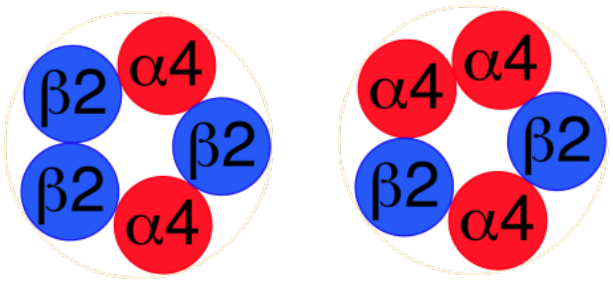


Higher sensitivity Lower sensitivity

Figure 1-2. The two stoichiometries of the α4β2 nAChR receptor.

***The discovery of lynx1***

The lynx1 protein is a member of the ly-6/PLAUER superfamily, and expressed throughout the mammalian brain and peripheral nervous system (Miwa et al., 1999). It shares structural homology with snake venom toxins such as α-bungarotoxin, but is GPI-anchored. Addition of lynx1 to heterologously expressed α4β2 results in decreased sensitivity to ACh, while lynx1-KO mice display hypersensitivity to nicotine and improved learning and memory (Miwa et al., 2006). Data published thus far are consistent with a mechanism of lynx1 that would be expected of a GPI-anchored competitive antagonist binding to nAChRs at the plasma membrane (Miwa et al., 2011), depicted in Figure 1-3. Chapter two of this thesis develops the hypothesis that lynx1 might act intracellularly, in the endoplasmic reticulum, to influence the assembly of the α4β2 nAChR, thereby biasing the stoichiometry of the population of receptors reaching the plasma membrane.

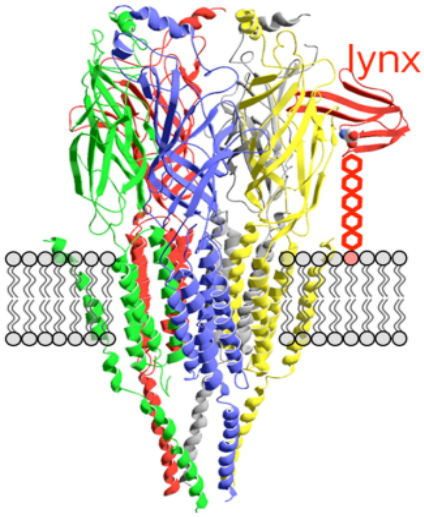


Figure 1-3. A model of lynx1 binding to a nAChR on the plasma membrane at the agonist-binding site.

***Epilepsy and ADNFLE***

Epilepsy is defined as having multiple incidences of seizure, and affects 1-2% of the population. While epilepsy is generally thought to result from hypersynchrony of neural firing, individual patients likely have differing pathophysiology and brain regions affected. Autosomal dominant nocturnal frontal lobe epilepsy (ADNFLE) is a rare monogenic form of epilepsy with a prevalence rate lower than 1 in 100,000. ADNFLE was the first form of epilepsy linked to genetic mutation in the nAChR α4 subunit (Steinlein et al., 1995). Since then, several other mutations in nAChR subunits have been associated with a high penetrance of ADNFLE. Chapter three of this thesis develops the hypothesis that at least one of the these mutations might cause ADNFLE by both increasing the sensitivity of α4β2, and altering the stoichiometry of α4β2 and α5α4β2 receptors on the plasma

membrane through biased assembly in the endoplasmic reticulum, and thus apparent in experiments on heterologous expression systems.

# References

Addington, J., and Addington, D. (1993). Premorbid functioning, cognitive functioning, symptoms and outcome in schizophrenia. Journal of Psychiatry and Neuroscience *18*, 18.

Bierut, L.J., Stitzel, J.A., Wang, J.C., Hinrichs, A.L., Grucza, R.A., Xuei, X., Saccone, N.L., Saccone, S.F., Bertelsen, S., Fox, L.*, et al.* (2008). Variants in nicotinic receptors and risk for nicotine dependence. Am J Psychiatry *165*, 1163-1171.

Buisson, B., and Bertrand, D. (2001). Chronic exposure to nicotine upregulates the human a4b2 nicotinic acetylcholine receptor function. J Neurosci *21*, 1819-1829.

Cahill, K., Stevens, S., Perera, R., and Lancaster, T. (2013). Pharmacological interventions for smoking cessation: an overview and network meta-analysis. Cochrane Database Syst Rev *5*.

Corey, E., Loh, T.P., AchyuthaRao, S., Daley, D.C., and Sarshar, S. (1993). Stereocontrolled total synthesis of (+)-and (-)-epibatidine. The Journal of Organic Chemistry *58*, 5600-5602.

Decker, M.W., Meyer, M.D., and Sullivan, J.P. (2001). The therapeutic potential of nicotinic acetylcholine receptor agonists for pain control. Expert opinion on investigational drugs *10*, 1819-1830.

Dilsaver, S.C., Snider, R.M., and Alessi, N.E. (1986). Stress induces supersensitivity of a cholinergic system in rats. Biological psychiatry *21*, 1093-1096.

Dunbar, G. (2010). Positive effects of the nicotinic channel blocker TC-5214 as augmentation treatment in patients with major depressive disorder who are inadequate responders to a first-line SSRI. Paper presented at: Journal of Psychopharmacology (SAGE PUBLICATIONS LTD 1 OLIVERS YARD, 55 CITY ROAD, LONDON EC1Y 1SP, ENGLAND).

Erhart, S.M., Marder, S.R., and Carpenter, W.T. (2006). Treatment of schizophrenia negative symptoms: future prospects. Schizophrenia Bulletin *32*, 234-237.

Fowler, C.D., Lu, Q., Johnson, P.M., Marks, M.J., and Kenny, P.J. (2011). Habenular α5 nicotinic receptor subunit signalling controls nicotine intake. Nature.

Freedman, R., Hall, M., Adler, L.E., and Leonard, S. (1995). Evidence in postmortem brain tissue for decreased numbers of hippocampal nicotinic receptors in schizophrenia. Biological psychiatry *38*, 22-33.

Gault, L., Ritchie, C., Robieson, W., Pritchett, Y., Othman, A., and Lenz, R. (2013). Efficacy and safety of the alpha7 agonist ABT-126 in mild-to-moderate Alzheimer's dementia. Alzheimer's & Dementia: The Journal of the Alzheimer's Association *9*, P138-P138.

Glassman, A.H., Helzer, J.E., Covey, L.S., Cottler, L.B., Stetner, F., Tipp, J.E., and Johnson, J. (1990). Smoking, smoking cessation, and major depression. Jama *264*, 1546-1549.

Gonzales, D., Rennard, S.I., Nides, M., Oncken, C., Azoulay, S., Billing, C.B., Watsky, E.J., Gong, J., Williams, K.E., and Reeves, K.R. (2006). Varenicline, an a4b2 nicotinic acetylcholine receptor partial agonist, vs sustained-release bupropion and placebo for smoking cessation: a randomized controlled trial. JAMA *296*, 47-55.

Gotti, C., Zoli, M., and Clementi, F. (2006). Brain nicotinic acetylcholine receptors: native subtypes and their relevance. Trends Pharmacol Sci *27*, 482-491.

Hall, S.M., Reus, V.I., Munoz, R.F., Sees, K.L., Humfleet, G., Hartz, D.T., Frederick, S., and Triffleman, E. (1998). Nortriptyline and cognitive-behavioral therapy in the treatment of cigarette smoking. Archives of general psychiatry *55*, 683-690.

Hansen, S.B., Sulzenbacher, G., Huxford, T., Marchot, P., Bourne, Y., and Taylor, P. (2006). Structural characterization of agonist and antagonist-bound acetylcholine-binding protein from Aplysia californica. J Mol Neurosci *30*, 101-102.

Hernan, M.A., Takkouche, B., Caamano-Isorna, F., and Gestal-Otero, J.J. (2002). A meta-analysis of coffee drinking, cigarette smoking, and the risk of Parkinson's disease. Ann Neurol *52*, 276-284.

Hu, M., Gopalakrishnan, M., and Li, J. (2009). Positive allosteric modulation of α7 neuronal nicotinic acetylcholine receptors: lack of cytotoxicity in PC12 cells and rat primary cortical neurons. British journal of pharmacology *158*, 1857-1864.

Hurt, R.D., Sachs, D.P., Glover, E.D., Offord, K.P., Johnston, J.A., Dale, L.C., Khayrallah, M.A., Schroeder, D.R., Glover, P.N., and Sullivan, C.R. (1997). A comparison of sustained-release bupropion and placebo for smoking cessation. New England Journal of Medicine *337*, 1195-1202.

Kabbani, N. (2008). Proteomics of membrane receptors and signaling. Proteomics *8*, 4146-4155.

Kesingland, A., Gentry, C., Panesar, M., Bowes, M., Vernier, J.-M., Cube, R., Walker, K., and Urban, L. (2000). Analgesic profile of the nicotinic acetylcholine receptor agonists,(+)-epibatidine and ABT-594 in models of persistent inflammatory and neuropathic pain. Pain *86*, 113-118.

Leslie, F.M., Mojica, C.Y., and Reynaga, D.D. (2013). Nicotinic receptors in addiction pathways. Molecular pharmacology *83*, 753-758.

Levin, E.D. (2002). Nicotinic receptor subtypes and cognitive function. J Neurobiol *53*, 633-640.

Lieberman, J.A., Dunbar, G., Segreti, A.C., Girgis, R.R., Seoane, F., Beaver, J.S., Duan, N., and Hosford, D.A. (2013). A randomized exploratory trial of an alpha-7 nicotinic receptor agonist (TC-5619) for cognitive enhancement in schizophrenia. Neuropsychopharmacology *38*, 968-975.

Lippiello, P.M., Beaver, J.S., Gatto, G.J., James, J.W., Jordan, K.G., Traina, V.M., Xie, J., and Bencherif, M. (2008). TC-5214 (S-(+)-Mecamylamine): A Neuronal Nicotinic Receptor Modulator with Antidepressant Activity. CNS neuroscience & therapeutics *14*, 266-277.

Lipska, B.K., and Weinberger, D.R. (2000). To model a psychiatric disorder in animals: schizophrenia as a reality test. Neuropsychopharmacology *23*, 223-239.

Luntz-Leybman, V., Bickford, P.C., and Freedman, R. (1992). Cholinergic gating of response to auditory stimuli in rat hippocampus. Brain Res *587*, 130-136.

Mansvelder, H.D., and McGehee, D.S. (2000). Long-term potentiation of excitatory inputs to brain reward areas by nicotine. Neuron *27*, 349-357.

Mineur, Y.S., Einstein, E.B., Seymour, P.A., Coe, J.W., O'Neill B, T., Rollema, H., and Picciotto, M.R. (2011). α4β2 nicotinic acetylcholine receptor partial agonists with low intrinsic efficacy have antidepressant-like properties. Behavioural pharmacology *22*, 291-299.

Miwa, J.M., Freedman, R., and Lester, H.A. (2011). Neural systems governed by nicotinic acetylcholine receptors: emerging hypotheses. Neuron *70*, 20-33.

Miwa, J.M., Ibanez-Tallon, I., Crabtree, G.W., Sanchez, R., Sali, A., Role, L.W., and Heintz, N. (1999). lynx1, an endogenous toxin-like modulator of nicotinic acetylcholine receptors in the mammalian CNS. Neuron *23*, 105-114.

Miwa, J.M., Stevens, T.R., King, S.L., Caldarone, B.J., Ibanez-Tallon, I., Xiao, C., Fitzsimonds, R.M., Pavlides, C., Lester, H.A., Picciotto, M.R.*, et al.* (2006). The Prototoxin lynx1 Acts on Nicotinic Acetylcholine Receptors to Balance Neuronal Activity and Survival In Vivo. Neuron *51*, 587-600.

Miyazawa, A., Fujiyoshi, Y., and Unwin, N. (2003). Structure and gating mechanism of the acetylcholine receptor pore. Nature *423*, 949-955.

Overstreet, D., and Russell, R. (1982). Selective breeding for diisopropyl fluorophosphate-sensitivity: behavioural effects of cholinergic agonists and antagonists. Psychopharmacology *78*, 150-155.

Overstreet, D.H. (1993). The Flinders sensitive line rats: a genetic animal model of depression. Neuroscience & Biobehavioral Reviews *17*, 51-68.

Pandya, A.A., and Yakel, J.L. (2013). Effects of neuronal nicotinic acetylcholine receptor allosteric modulators in animal behavior studies. Biochemical pharmacology *86*, 1054-1062.

Picciotto, M.R., Addy, N.A., Mineur, Y.S., and Brunzell, D.H. (2008). It is not "either/or": Activation and desensitization of nicotinic acetylcholine receptors both contribute to behaviors related to nicotine addiction and mood. Prog Neurobiol *84*, 329-342.

Pons, S., Fattore, L., Cossu, G., Tolu, S., Porcu, E., McIntosh, J.M., Changeux, J.P., Maskos, U., and Fratta, W. (2008). Crucial role of α4 and α6 nicotinic acetylcholine receptor subunits from ventral tegmental area in systemic nicotine self-administration. J Neurosci *28*, 12318-12327.

Prickaerts, J., van Goethem, N.P., Chesworth, R., Shapiro, G., Boess, F.G., Methfessel, C., Reneerkens, O.A., Flood, D.G., Hilt, D., and Gawryl, M. (2012). EVP-6124, a novel and selective α7 nicotinic acetylcholine receptor partial agonist, improves memory performance by potentiating the acetylcholine response of α7 nicotinic acetylcholine receptors. Neuropharmacology *62*, 1099-1110.

Pucilowski, O., Overstreet, D.H., Rezvani, A.H., and Janowsky, D.S. (1993). Chronic mild stress-induced anhedonia: greater effect in a genetic rat model of depression. Physiology & behavior *54*, 1215-1220.

Rabenstein, R., Caldarone, B., and Picciotto, M. (2006). The nicotinic antagonist mecamylamine has antidepressant-like effects in wild-type but not β2-or α7-nicotinic acetylcholine receptor subunit knockout mice. Psychopharmacology *189*, 395-401.

Roth, B.L., Sheffler, D.J., and Kroeze, W.K. (2004). Magic shotguns versus magic bullets: selectively non-selective drugs for mood disorders and schizophrenia. Nat Rev Drug Discov *3*, 353-359.

SalÃn-Pascual, R.J., Rosas, M., Jimenez-Genchi, A., and Rivera-Meza, B.L. (1996). Antidepressant effect of transdermal nicotine patches in nonsmoking patients with major depression. Journal of Clinical Psychiatry.

Seeman, P. (2002). Atypical antipsychotics: mechanism of action. Canadian journal of psychiatry Revue canadienne de psychiatrie *47*, 27-38.

Spande, T.F., Garraffo, H.M., Edwards, M.W., Yeh, H.J., Pannell, L., and Daly, J.W. (1992). Epibatidine: a novel (chloropyridyl) azabicycloheptane with potent analgesic activity from an Ecuadoran poison frog. Journal of the American Chemical Society *114*, 3475-3478.

Steinlein, O.K., Mulley, J.C., Propping, P., Wallace, R.H., Phillips, H.A., Sutherland, G.R., Scheffer, I.E., and Berkovic, S.F. (1995). A missense mutation in the neuronal nicotinic acetylcholine receptor a4 subunit is associated with autosomal dominant nocturnal frontal lobe epilepsy. Nat Genet *11*, 201-203.

Swope, S.L., Qu, Z., and Huganir, R.L. (1995). Phosphorylation of the Nicotinic Acetylcholine Receptor by Protein Tyrosine Kinasesa. Annals of the New York Academy of Sciences *757*, 197-214.

Tang, J., and Dani, J.A. (2009). Dopamine enables in vivo synaptic plasticity associated with the addictive drug nicotine. Neuron *63*, 673-682.

Tanner, C.M., Goldman, S.M., Aston, D.A., Ottman, R., Ellenberg, J., Mayeux, R., and Langston, J.W. (2002). Smoking and Parkinson's disease in twins. Neurology *58*, 581-588.

Unwin, N. (2005). Refined Structure of the Nicotinic Acetylcholine Receptor at 4A Resolution. J Mol Biol *346*, 967-989.

Williams, D.K., Peng, C., Kimbrell, M.R., and Papke, R.L. (2012). Intrinsically low open probability of α7 nicotinic acetylcholine receptors can be overcome by positive allosteric modulation and serum factors leading to the generation of excitotoxic currents at physiological temperatures. Molecular pharmacology *82*, 746-759.

Williams, D.K., Wang, J., and Papke, R.L. (2011). Positive allosteric modulators as an approach to nicotinic acetylcholine receptor-targeted therapeutics: advantages and limitations. Biochemical pharmacology *82*, 915-930.

Williams, J.M., Ziedonis, D.M., Abanyie, F., Steinberg, M.L., Foulds, J., and Benowitz, N.L. (2005). Increased nicotine and cotinine levels in smokers with schizophrenia and schizoaffective disorder is not a metabolic effect. Schizophrenia research *79*, 323-335.

Zwart, R., and Vijverberg, H.P. (1998). Four Pharmacologically Distinct Subtypes of α4β2 Nicotinic Acetylcholine Receptor Expressed in Xenopus laevisOocytes. Molecular pharmacology *54*, 1124-1131.

# Chapter II:
# Lynx1 shifts α4β2 nicotinic receptor subunit stoichiometry by affecting assembly in the endoplasmic reticulum*

*This chapter has been submitted as a manuscript to The Journal of Biological Chemistry by the authors Weston A. Nichols, Brandon J. Henderson, Caroline Yu, Rell L. Parker, Christopher I. Richards, Henry A. Lester, and Julie M. Miwa.

# Abstract

GPI-anchored neurotoxin-like receptor binding proteins, such as lynx modulators, are topologically positioned to exert pharmacological effects by binding to the extracellular portion of nAChRs. These actions are generally thought to proceed when both lynx and the nAChRs are on the plasma membrane. Here, we demonstrate that lynx1 also exerts effects on α4β2 nAChRs within the endoplasmic reticulum. Lynx affects assembly of nascent α4 and β2 subunits, and alters the stoichiometry of the population that reaches the plasma membrane. Additionally, these data suggest that lynx1 alters nAChR stoichiometry primarily through this intracellular interaction, rather than via effects on plasma membrane nAChRs. To our knowledge, these data represent the first test of the hypothesis that a lynx family member, or indeed any GPI-anchored protein, could act within the cell to alter assembly of multi-subunit protein.

# Introduction

Cholinergic systems are involved in diverse functions including mood, anxiety, learning and memory, addiction, and movement disorders (Miwa et al., 2011). The nicotinic acetylcholine receptors (nAChRs) of the cholinergic system are comprised of 15 different subunits (α1-10 and β1-4) which assemble into both homopentameric receptors such as $(\alpha7)_5$ or $(\alpha9)_5$ and heteropentameric receptors such as α4β2 (Jensen et al., 2005). Subunit composition, and even the position of specific subunits within pentamers, can influence the biophysical, pharmacological, and cell biological properties of the receptor, with profound effects on information processing in neurons that express these nAChRs (Gotti et al., 2009).

Subunit composition influences the properties of the two possible pentameric stoichiometries of α4β2 nAChRs, the most abundant heteromeric nAChR subtype in the brain. In a terminology that emphasizes their differences with respect to acute pharmacology, the $(\alpha4)_3(\beta2)_2$ receptors are known as low sensitivity (LS) receptors, while $(\alpha4)_2(\beta2)_3$ receptors are known as high sensitivity or (HS) receptors (Moroni et al., 2006) (Gotti et al., 2009). These two stoichiometries exhibit different desensitization kinetics and respond differently to chronic nicotine treatment. HS receptors are upregulated in response to nicotine, while LS receptors are unaffected. This is thought to play an important role in mechanisms of nicotine addiction (Nelson et al., 2003; Srinivasan et al., 2014). Additionally, subunit composition could possibly influence sub-cellular localization of receptors on the plasma membrane (PM).

The lynx family proteins are a subset of the Ly6/uPAR superfamily. This superfamily is related to the elapid snake venom toxin genes, such as α-bungarotoxin,

consisting of a three-fingered folding motif and multiple internal disulfide bonds (Lyukmanova et al., 2011; Miwa et al., 1999). α-bungarotoxin and other such toxins exemplify a highly conserved receptor binding motif which is also carried over to lynx proteins (Lyukmanova et al., 2011; Miwa et al., 1999; Miwa et al., 2012). α-bungarotoxin and other toxins have become widely used probes for the investigation of the properties of nAChR. Snakes inject these toxins into their prey; in contrast, the role of a toxin-like molecule expressed within a cell together with nAChRs has not been widely studied. Since the discovery of lynx1, many other lynx family members have been found, and several include GPI anchors (Chimienti et al., 2003; Miwa et al., 2011; Miwa et al., 2012). The GPI-linked lynx1 and lynx2 molecules are presumably present in membranes early in the exocytotic pathway, such as the endoplasmic reticulum (ER). Therefore, the existence of the GPI-anchor on lynx1 and lynx2 proteins could contribute to the structure, composition, or function of nascent nAChRs as well.

The differential contributions of lynx genes to brain function are influenced to a large degree by the regions of expression. For instance, lynx1 is widely expressed throughout the brain, with high levels in the cerebral cortex and hippocampus, playing a role in learning and neuronal plasticity (Miwa et al., 2006; Miwa and Walz, 2012; Morishita et al., 2010). The lynx2 gene, in contrast, has a more restricted expression with high levels in the fear/anxiety structure of the amygdala, and lynx2 KO mice display elevated fear and anxiety-related behaviors (Tekinay et al., 2009). Selectivity for nAChR subtypes (α7 and β2 nAChRs) have also been found for lynx1 proteins, and could provide another level of regulation as yet not well explored.

GPI-anchored neurotoxin-like receptor binding proteins, such as lynx modulators, are confined to a volume just a few nanometers above the extracellular face of the membrane. This topology positions them to exert pharmacological effects by binding to the extracellular portion of nAChRs. These actions have previously been thought to proceed on the PM. Among the pharmacological effects of small-molecule ligands is pharmacological chaperoning of α4β2 nAChRs; this proceeds when the ligands enter the ER (Srinivasan et al., 2014) and, perhaps, the Golgi (Henderson et al., 2014). Thus far, there have been no reports of lynx modulators exerting an effect inside cells. Here, we investigated the hypothesis that lynx1 also exerts an effect on α4β2 nAChRs within the endoplasmic (ER) reticulum. To our knowledge, these data represent the first report of a lynx family member, or indeed any GPI-anchored protein, acting within the cell to alter assembly of multi-subunit proteins.

# Experimental Procedures

### *Plasmid Constructs*

Mouse lynx1 cDNAs including an N-terminally fused fluorescent tag (eGFP, mCherry, or SEP) were constructed by PCR amplification using the forward primer 5′-gcctgcctgtggcccaggctatggtgagcaagggcgag-3′ and the reverse primer 5′-aggcacacacgtggcactccagcttgtacagctcgtccatgcc-3′, which overlap with both sequences before and after the N-terminal signal sequence of the lynx1-coding sequence (Figure 2-1A). Four XFP-lynx1 constructs were made with four different linkers separating the fluorescent tag from mature lynx1: 1. no linker, 2. Gly-Ser, 3. Gly-Gly-Ser-Gly, or 4. Tyr-Ser-Asp-Leu (YSDL). All experiments presented in this paper utilize the YSDL linker version of the construct because it has been used previously with another GPI-linked fusion protein, GFP-CD59 (Kenworthy, 2004; Nichols et al., 2001, and Prasanna Satpute and Jennifer Lippincott-Schwartz, personal communication), and it was the first construct we validated via electrophysiology. This PCR product was then cloned directly into the vector containing the lynx1 gene using Pfu-Turbo polymerase.

We used mouse α4-wt, α4-GFP, α4-mCherry, β2-wt, β2-GFP, and β2-mCherry cDNA clones inserted into pCI-NEO vectors as described previously (Nashmi et al., 2003).

### *Tissue Culture and Transfection*

Mouse neuroblastoma-2a (N2a) cells were cultured using standard techniques and maintained in DMEM (Invitrogen) supplemented with 10% FBS. N2a cells were plated by adding 90,000 cells to poly-d-lysine-coated 35-mm glass-bottom imaging dishes (MatTek, Ashland, MA). The next day, plasmid DNA was mixed with cationic lipids by adding 500-

750 ng of each nAChR plasmid and lynx1 construct to 4 μl of Lipofectamine 2000 transfection reagent in 200 μl of OptiMEM (Invitrogen). After 20 min at room temperature, the transfection mixture was added to N2a cells in 1 ml of plating medium and incubated at 37 °C for 24 h. Dishes were rinsed twice with plating medium and incubated at 37 °C for an additional 24 h before imaging or electrophysiological experiments. HEK293 cells were also cultured using standard cell techniques as detailed above. N2A cells and HEK293 cells were obtained from ATCC (Manassas, VA).

Primary mouse E16.5 neurons were extracted from mouse embryos and plated on 35-mm polylysine-coated glass bottom culture dishes (Mattek) in a neuronal medium containing Neurobasal, B27 (Invitrogen), and Glutamax supplemented with 3% equine serum. We defined this initial plating as day-in-vitro zero (div 0). Neurons were plated at a density of 60,000 cells per dish. On div 4, neurons were treated with 1 μM cytosine arabinoside to halt the division of glial cells. Neurons were maintained via 50% exchange with feeding medium (Neurobasal, B27, and Glutamax) twice per week. On div 9, plasmids were mixed in 100 μl of OptiMEM, and 4 μl of Lipofectamine-2000 was mixed with a separate 100-μl aliquot of OptiMEM. After 5 min at room temperature, the separate solutions were mixed together and kept at room temperature for an additional 25 min. Neurons were transfected with 750 ng of each nAChR plasmid and of XFP-lynx1 plasmid. After 3 h at 37 °C, transfection medium was replaced with neuronal feeding medium. Neurons were imaged on day in vitro (div) 10.

***Co-immunoprecipitation***

HEK293 cells were plated (on day 1) at a density of 4 million cells per 10 cm dish. Cells were transfected on day 2 with 5 μg of each construct DNA using ExpressFect reagent (Denville Scientific, South Plainfield, NJ) according to the manufacturer's protocol. On day 3, medium was aspirated gently and replaced with fresh growth medium. Cells were harvested on day 4 by removing cells from 37 °C incubator, placing on ice, scraping cells from dish with a cell scraper (Corning Inc., Corning, NY), and transferring cells to a 15 mL conical tube for centrifugation and lysis. Cells were lysed in 1 mL of ice-cold NP40 extraction buffer (50 mM Tris, pH 7.4, 50 mM NaCl, 1% NP40, 1 mM EDTA, 1 mM EGTA, 1% P8340 and 4 mM phenylmethylsulfonyl fluoride (PMSF)) by gently pipetting up and down 25 times. Cell lysate was centrifuged for 5 min at 4 °C and then combined with preformed complexes of protein A Dynabeads (Invitrogen, Carlsbad, CA) and rabbit-anti-GFP antibody (A11122, Molecular Probes, Invitrogen) for immunoprecipitation at room temperature on a rocker for 1 h. Dynabead-antibody-antigen complexes were removed from the supernatant via magnet, and washed. Complexes were dissociated by incubating in reducing buffer (50% Laemmli sample buffer, BIO-RAD, Hercules, CA) for 10 min at 70 °C. Dissociated samples were removed from beads via magnet, allowed to cool on ice, and loaded into an SDS-PAGE gel for Western blot analysis.

***Western Blot***

Samples were run on an SDS-PAGE protein gel, transferred to a nitrocellulose membrane, blocked with blocking buffer (TBS with 0.1% Tween-20 + 5% dry milk), and probed with goat-anti-lynx primary antibody (sc-23060, Santa Cruz Biotechnology, Santa

Cruz, CA). Of three antibody lots purchased from the supplier, only one gave satisfactory results; unfortunately that lot is no longer available. Membranes were probed with secondary IR800-anti-goat antibody (926-32214, Li-Cor Biosciences, Lincoln, NE). Membranes were then imaged in an Odyssey near infrared imager (Li-Cor Biosciences).

***Confocal Microscopy***

N2a cells and neurons were imaged as described previously (Drenan et al., 2008; Moss et al., 2009) in L15 Buffer (150 mM NaCl, 4 mM KCl, 2 mM $CaCl_2$, 2 mM $MgCl_2$, 10 mM HEPES, and 10 mM D-glucose, pH 7.4), a $CO_2$ independent media. Briefly, cells were imaged with a Nikon (Nikon Instruments, Melville, NY) C1 laser-scanning confocal microscope system equipped with spectral imaging capabilities and a Prior (Rockland, ME) remote-focus device, and a Nikon Plan Apo 60X 1.40 NA oil objective. Pinhole diameter was 30-60 μm, and cells were imaged at 12-bit intensity resolution over 512 × 512 pixels at a pixel dwell time 6.72 μs. GFP was excited using a 488 nm modulated diode laser, and mCherry was excited with an argon laser at 561 nm. In most cases, imaging was carried out using the Nikon C1si DEES grating and spectral detector with 32 parallel photomultiplier tubes. This allowed us to collect spectral images (λ stacks). In such images, each pixel of the X-Y image contains a list of emission intensity values across a range of wavelengths. We collected light at wavelength intervals between 485 and 650 nm, at steps of 5 nm. We used the Nikon EZC1 linear unmixing algorithm to reconstruct GFP and mCherry images. For each pixel of a spectral image, intensity of GFP and mCherry was determined from fluorescence intensity values at the peak emission wavelength derived from the reference spectra.

Phosphotidylinositol-specific phospholipase C (PI-PLC) (CAS #: 37288-19-0, Product #: P8804, Sigma-Aldrich) was used to cleave the GPI-anchor of lynx1, and thus cleave the protein from the PM. After addition of 0.25 units/mL of PI-PLC to cell culture dish, cells were incubated for 1 h at 37 °C either in a mammalian cell incubator or within a climate-controlled chamber on the microscope stage (for before and after images). After PI-PLC treatment, cells were briefly washed twice with 2 ml of fresh medium and subsequently imaged. An aqueous glycerol solution buffer of 60% v/v glycerol, 10 mM Tris HCl, 10 mM EDTA, at a pH of 8.0 was used as a control with no PI-PLC enzyme.

***Measuring FRET with Donor Recovery After Photobleaching (DRAP)***

To examine FRET between various nAChR subunits, the acceptor photobleaching method was used with a modified fluorescence recovery after photobleaching macro built into the Nikon EZC1 imaging software, as described previously (Drenan et al.). In this method, FRET was detected by recording GFP signal increases during incremental photodestruction of mCherry. A spectral image was acquired once before mCherry bleaching and at six time points during mCherry bleaching at 561 nm. Laser power during bleaching was constant at 80%. One bleach scan per cycle was used. This bleaching protocol was optimized to achieve 75 to 90% photodestruction of mCherry while still enabling us to record incremental increases in GFP emission at each time point. To measure FRET, spectral images were unmixed into their GFP and mCherry components as described above. We measured GFP and mCherry mean intensity throughout the entire cell by selecting the cell perimeter as the boundary of a region of interest in Nikon's EZC1 software. GFP and mCherry components were saved in Excel format, and fluorescence

intensities were normalized to the pre-bleach time point (100%). FRET efficiency ($E$) was calculated as $E = 1 - (I_{DA}/I_D)$, where $I_{DA}$ represents the normalized fluorescence intensity of GFP (100%) in the presence of both donor (GFP) and acceptor (mCherry), and $I_D$ represents the normalized fluorescence intensity of GFP in the presence of donor only (complete photo-destruction of mCherry). The $I_D$ value was extrapolated from a scatter plot of the fractional increase of CFP versus the fractional decrease of YFP. The $E$ values were averaged from several cells per condition.

***Mammalian Cell Electrophysiology***

N2a cells were co-transfected with nAChR subunits tagged with eGFP to facilitate visual identification of transfected cells. We used an inverted fluorescence microscope (IX71, Olympus) equipped with an Hg lamp (HB-10103AF, Nikon) to visualize the fluorescent cells. Whole-cell voltage-clamp currents were recorded using an Axopatch-1D amplifier (Axon Instruments) and digitized with a Digidata 1440A analog-to-digital converter (Axon) under the control of pClamp 10.0 software (Axon). The pipette solution contained (in mM): 135 K gluconate, 5 KCl, 5 EGTA, 0.5 $CaCl_2$, 10 HEPES, 2 Mg-ATP, and 0.1 GTP, pH adjusted to 7.2 with Tris-base, osmolarity to 280-300 mOsm with sucrose). Electrode resistance was 2-6 MΩ. All recordings were obtained at ambient temperature. Data were low-passed filtered at 2 kHz and sampled at 10 kHz. ACh was dissolved in an extracellular solution containing (in mM): 140 NaCl, 5 KCl, 2 $CaCl_2$, 1 $MgCl_2$, 10 HEPES, and 10 glucose (320 mOsm, pH to 7.3 with Tris-base), and applied to cells using a Picospritzer (20 psi) or a commercially available microperfusion system (Octaflow II, ALA Scientific Instruments). The holding potential was -50 mV. To

minimize agonist-induced desensitization, we applied ACh at ~3 min intervals, and continually perfused the recording chamber with extracellular solution.

Phosphotidylinositol-specific phospholipase C (PI-PLC) was used to cleave lynx1 from the PM. We exposed cells to 0.25 units/mL for 1 h at 37 °C incubation prior to electrophysiology assays.

***Statistical Analysis***

Concentration-response relations for the ACh-induced fluorescent membrane potential changes and voltage-clamp currents were fit to the Hill equation using nonlinear least-squares regression (OriginLab software). Errors reported for the mean values are ± SEM. Statistical significance was determined by either Student's t test or by one-way analysis of variance (ANOVA) where multiple pairwise comparisons were conducted. Significant differences are reported at the level of $p<0.05$ (*), $p<0.01$ (**), or $p<0.001$ (***).

# Results

***Construction of XFP-lynx1 reveals subcellular localization both on the plasma membrane and in the endoplasmic reticulum.***

We constructed four variants of the mCherry-lynx1 construct, each with a unique linker as described in Methods. The mCherry was inserted after the N-terminal signal sequence and before the mature lynx1 protein sequence as shown in Figure 2-1A. All four variants are fluorescent, indicating that the mCherry fluorophore folds properly. We proceeded with electrophysiological validation of the construct with the YSDL linker (see Figures 2-3 and 2-5 below) because that particular linker had been previously characterized on a similar fluorescent GPI-linked fusion protein, GFP-CD59 (Nichols et al., 2001). After validation by electrophysiology, we made two additional constructs by replacing the mCherry sequence with that of GFP or superecliptic pHluorin (SEP). To test the similarity of the GFP and mCherry constructs, we co-transfected them together into cultured mouse E16.5 cortical neurons (Figure 2-1B). Both constructs show a patchy, segmented appearance. We compared this distribution to that of two other proteins. We co-transfected GFP-lynx1 with tau1-mCherry (Figure 2-1D). The tau1-mCherry localizes to microtubules, allowing visualization of processes to determine whether they are segments. We found that most of the neurons in the dish had less patchy tau1-mCherry fluorescence than GFP-lynx1 fluorescence, suggesting that lynx1 may normally be present in clusters within cells. This may be due to the GPI–anchor interacting with specific cholesterol-rich membrane domains. When co-transfected with GalT-mCherry, GFP-lynx1 showed little overlap (Figure 2-1E), indicating that most lynx1 molecules did not reside in the trans-Golgi network.

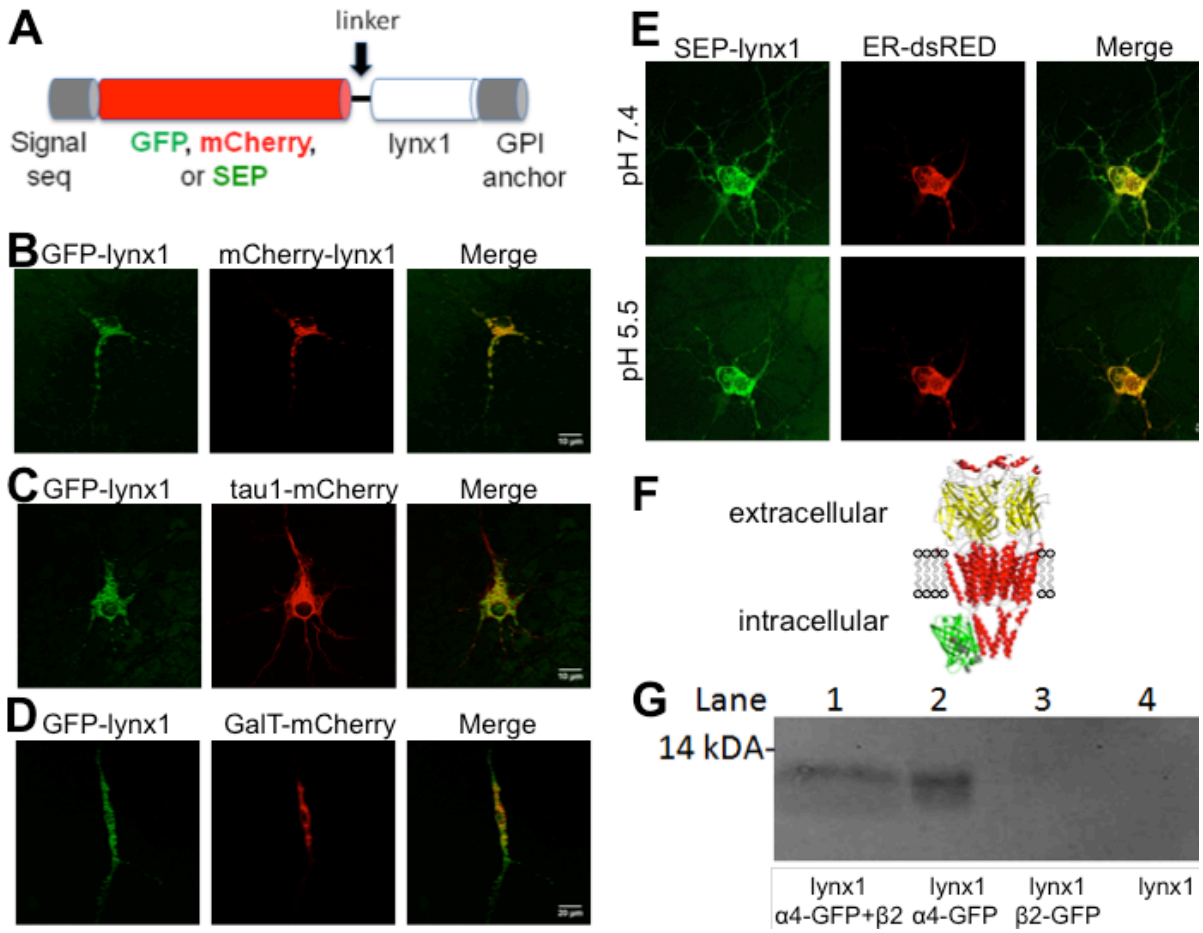


Figure 2-2. Lynx1 is present in ER in addition to the PM. A. Construction of fluorescently-tagged lynx1 constructs, schematic of GFP, mCherry or SEP insertion after the N-terminal signal sequence of lynx1. B-E, mouse E16.5 neurons transfected with various fluorescently-tagged proteins. B, both GFP-lynx1 and mCherry-lynx1. C, GFP-lynx1 and tau1-mCherry, a marker for microtubules, partially colocalize. D, GFP-lynx1 and GalT-mCherry, indicating that the majority of lynx1 is outside the Golgi. E, SEP-lynx1 and ER-dsRED, at both pH 7.4 and 5.5. Quenching at pH 5.5 indicates that lynx1 is present both in the ER and on the plasma membrane. F, Topology of an α4- or β2-GFP construct. α4- or β2-GFP nAChRs were labeled with a genetically encoded GFP inserted into the intracellular M3-M4 loop. The cartoon of nAChR derives from PDB 2BG9, and the cytoplasmic portions are incomplete. G, Co-immunoprecipitation indicates that lynx1 binds and forms stable complexes with α4-GFP both with β2 present (lane 1) and with no other nAChR subunits present (lane 2). α4 subunits alone are unable to leave the ER, thus lynx1 must bind in the ER. lynx1 was not detectable when either co-transfected with β2-GFP (lane 3), or alone (lane 4).

SEP is a pH-sensitive version of GFP with a pKa of ~ 7.0. SEP is fluorescent at pH 7.4, but is quenched at pH < 7.0 (Miesenböck et al., 1998). SEP provides information about the percentage of receptors that are present on the PM when linked to the extracellular portion of Cys-loop receptors (Henderson et al., 2014; Jacob et al., 2005; Khiroug et al., 2009; Richards et al., 2011) and other membrane proteins. We used this pH dependence to visualize and discriminate between SEP-lynx1 molecules residing intracellularly vs. those residing on the PM, as shown in Figure 2-1E. When the pH was adjusted to 5.4 by perfusion, we observed that fluorescence decreased but did not disappear, suggesting that a population of SEP-lynx1 resides on the PM and a portion resides in the ER.

***Lynx1 binds α4-GFP in the ER***

Previous assays on HEK293T cells transfected with α4, β2 (both FLAG-tagged constructs), and lynx1, immunoprecipitation of either α4 with anti-α4 antibody (mAb299), or immunoprecipitation of both α4 and β2 with anti-FLAG antibodies, showed co-immunoprecipitation of nAChRs with lynx1 (Ibanez-Tallon et al., 2002). Here, we demonstrate that lynx1 and α4 also co-immunoprecipitate when the β2 subunit is omitted (Figure 2-1F). Because α4 subunits alone do not form a complete, pentameric receptor, they do not efficiently leave the ER (Whiteaker et al., 1998).

To test whether lynx1 could bind the individual subunits of the α4β2 nAChR and potentially affect assembly we co-transfected either: (1) α4-GFP, β2-wt, and lynx1; (2) α4-GFP and lynx1; (3). β2-GFP and lynx1; or (4) lynx1 alone into HEK293 cells (Figure 2-1F, G). We probed for lynx1 after precipitating the nAChR subunits with an anti-GFP

antibody. We found that when α4 is present, either alone or with β2, lynx1 was pulled down. We could not detect lynx1 when β2-GFP precipitated down, or in the control where there was no nAChR subunit co-transfected (Figure 2-1G). Since it appears that lynx1 can bind the α4 subunit without the presence of β2, we conclude that lynx1 is able to bind to α4 before pentamers are formed, suggesting that association of lynx1 with α4 occurs in the ER.

***lynx1 stabilizes α4/α4 dimers, but not β2/β2 dimers, in the ER***

To measure whether the presence of lynx1 affects receptor formation we conducted four types of donor-recovery after photo-bleaching (DRAP) FRET experiments on mouse N2a cells transfected with nAChR subunits plus or minus lynx1 (Figure 2-2). We co-transfected α4-GFP, α4-mCherry, and either empty vector or lynx1(we did not co-transfect a β subunit). In this case, we measure DRAP between α4/α4 dimers in the ER, as α4 without a β subunit cannot assemble into a full pentamer and subsequently cannot efficiently exit the ER. The addition of lynx1 increased the FRET efficiency between these dimers from (6.7% ± 1.13%, 26 cells) to (14.59% ± 1.51%, 32 cells), suggesting that lynx1 binds α4 subunits in the ER, increasing dimerization and potentially assisting the formation of the LS stoichiometry (Figure 2-2A , B, and, E). In another series, we obtained FRET measurements between α4-GFP and α4-mCherry in the presence of β2-wt of (9.33% ± 0.85%, 40 cells) and (3.09% ± 1.11%, 36 cells) with empty vector and lynx, respectively. When we co-expressed fluorescently labeled β2 subunits, β2-GFP and β2-mCherry, either in the presence or absence of α4-wt, the addition of lynx1 did not significantly alter the FRET efficiency (Figure 2-2 B1-B2, C1-C2, E). For β2-GFP/β2-mCherry with no α4-wt or

lynx, the FRET efficiency was (25.1% ± 2.79%, 31 cells); when lynx was added, the FRET efficiency was 27.5% ± 2.4%, (24 cells). For β2-GFP/β2-mCherry with α4-wt, the FRET efficiencies were (18.4% ± 1.3%, 29 cells), and (18.5% ± 1.7%, 33 cells) for empty vector and lynx, respectively. Data are reported here as (mean ± S.E.M., number of cells per condition).

These data show that lynx1 increases the assembly of α4/α4 dimers and does not alter β2/β2 dimer assembly. To assess the effect of lynx1 on fully assembled α4β2 nAChR pentamers, we co-expressed α4-GFP, α4-mCherry, β2-wt, and either empty vector (pcDNA3.1) or lynx1. The addition of lynx1 increased the FRET between the fluorescently labeled α4 subunits, indicating that lynx1 increases the extent to which α4 subunits assemble together in complexes (Figure 2-2E). This shift could be due to increased incorporation of the α4 subunit into the auxiliary position of α4β2 fully formed pentamers (LS, $(\alpha4)_3(\beta2)_2$ stoichiometry). It could also be due to increased α4/α4 dimers in the ER. These two outcomes are not mutually exclusive, in fact, the latter (increased α4/α4 dimers in the ER) would likely lead to the former by biasing assembly towards the formation of $(\alpha4)_3(\beta2)_2$ (LS) nAChRs. This would presumably result in more LS receptors being exported from the ER and eventually trafficked to the PM.

A high baseline level of acceptor or low post-acceptor-bleaching level of donor could distort the measurements of FRET efficiency. To rule this out we calculated the ratio between GFP and mCherry expression (Figure 2-2F, G). We achieved ratios consistently between 0.6 to 2.0, which are within the acceptable range for DRAP measurements.

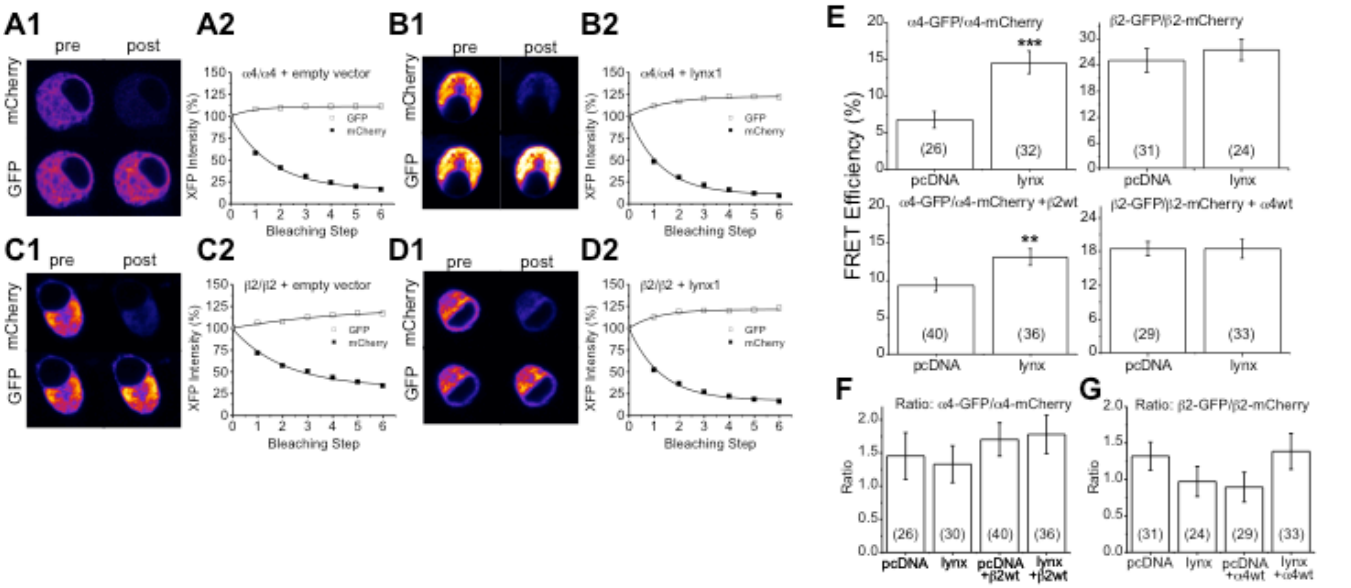


Figure 2-3. Donor recovery after photobleaching (DRAP). N2a cells were transfected with either α4-GFP and α4-mCherry (A1, A2, B1, and B2 show exemplar data) or β2-GFP and β2-mCherry (C1, C2, D1, and D2 show exemplar data). The acceptor fluorophore (mCherry) was photobleached, causing an increase in fluorescence of the donor fluorophore (GFP). α4-GFP and α4-mCherry were co-transfected either with empty vector or with lynx1. β2-GFP and β2-mCherry were co-transfected either with empty vector (C1-C2), or with lynx1 (D1-D2). Lynx1 increases FRET efficiency between α4 subunits, but not between β2 subunits. E, lynx1 increases FRET efficiency between α4-GFP and α4-mCherry subunits when no other subunits are present (top left) and also when co-transfected with β2 (bottom left). lynx1 does not increase FRET efficiency between fluorescently tagged β2 subunits either without α4 present (top right) or with co-transfected α4 (bottom right). F-G, lynx1 has no effect on the ratio of signals, GFP/mCherry for fluorescently tagged α4 (F) or β2 (G). Numbers within parentheses in bar graphs represent number of cells per condition.

***lynx1 causes a shift in population stoichiometry of the α4β2 nAChR on the plasma membrane***

Previous studies on lynx1 showed that lynx1 reduces the sensitivity of α4β2 receptors to ACh, both in heterologous expression systems and *in vivo* (Ibanez-Tallon et al., 2002; Miwa et al., 1999; Miwa et al., 2006). However, it has not been previously demonstrated that lynx1 shifts the stoichiometry of α4β2 receptors on the PM by biasing assembly of nascent subunits within the ER. To test this hypothesis, we completed a series of electrophysiology assays (Figure 2-3).These electrophysiological experiments examined the effect of lynx1 and fluorescently tagged XFP-lynx1 on α4β2. We transfected N2a cells with α4-GFP and β2-wt nAChR subunits and either lynx1 (wt or mCherry) or empty vector. The addition of lynx1-wt or mCherry-lynx1 reduced peak current sizes, reduced the proportion of HS receptors, and decreased the decay time (Figure 2-3, Table 1). Addition of lynx1-wt reduced α4β2 nAChR peak current amplitude to ~40% of the maximal response, (from 3280 ± 1320 pA [5 cells] to 1,060, ± 402 pA, [6 cells]) for lynx1-wt (Figure 2-3A, B, D). Addition of mCherry-lynx1 similarly reduced the α4β2 nAChR peak current amplitude to ~30% of the maximal response (539.4 ± 115 pA, 10 cells) (Figure 2-3A, C, D). There was no significant difference between lynx1-wt and mCherry-lynx1 in regards to mean peak current amplitude, decay time, or waveform (Figure 2-3D, E). This suggests that the addition of the mCherry fluorophore to lynx1 does not significantly alter its function.

Next we collected concentration-response data to assess changes in α4β2 nAChR stoichiometry. Previous assays have validated that the LS and HS α4β2 nAChR stoichiometries have distinct pharmacological profiles: LS nAChRs and HS nAChRs have different $EC_{50}$ values with ACh (~ 30μM and 3 μM, respectively) (Nelson et al., 2003; Tapia et al., 2007). Without lynx1, α4β2 nAChRs have a two-component dose-response relation, with a pronounced HS-like behavior at [ACh] ≤ 1 μM (Figure 2-3F). The addition of lynx1 (wt, or mCherry) produced less

pronounced responses at lower [ACh] (Figure 2-3F,). This suggests that in the presence of lynx1, the HS α4β2 nAChR population is decreased. Therefore, PM α4β2 nAChRs are composed mainly of LS α4β2 nAChRs. The Hill equation fits (Table 2-1) are consistent with a shift in components. In the absence of lynx1, ~50% of HS component (as often observed in α4β2 experiments); but in each of the lynx1 conditions this is reduced to ~25-28% HS. A compelling contrast is shown for the normalized data at 10 μM ACh (Figure 2-3G), which was chosen because this dose produces near maximal responses at HS receptors, with minimal contribution by LS receptor (Moroni et al., 2006; Nelson et al., 2003).

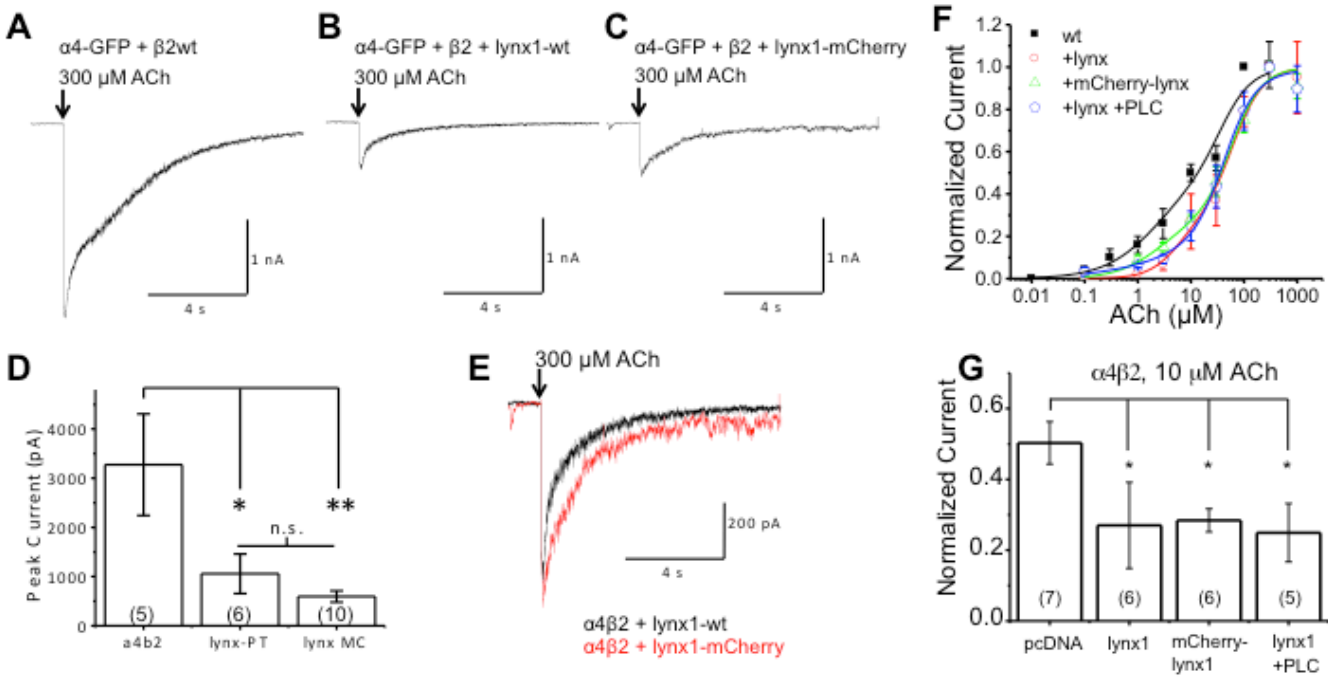


Figure 2-4. Electrophysiology in Neuroblastoma-2a cells: lynx1-wt and mCherry-lynx1 have similar effects on α4β2. A-C, sample traces from N2a cells transfected with α4-GFP, β2-wt, and either empty vector (A), lynx1-wt (B), or mCherry-lynx1 (C) where ACh was puffed for 100 ms. D, Both lynx1-wt and mCherry-lynx1 decrease peak currents at 300 μM ACh when compared to empty vector. E, traces from N2a cells when transfected with α4β2 and either lynx1-wt or mCherry-lynx1. F-G. Addition of lynx1 variants shifts the dose-response relation of α4β2 to the right, towards a greater proportion of the low-sensitivity $(\alpha4)_3(\beta2)_2$ stoichiometry. F, Dose-response curves of α4β2 when co-transfected with empty vector, lynx1, mCherry-lynx1, or lynx1 and treatment with phospholipase-C (PLC) for 1 h at 37 °C. G, Comparison of normalized current between α4β2 and lynx1 variant conditions at 10 μM ACh. 10 μM was selected to maximize activation of high-sensitivity ($EC_{50}$ ≈ 3 μM) stoichiometry $(\alpha4)_2(\beta2)_3$ receptors, while minimizing activation of the lower-sensitivity ($EC_{50}$ ≈ 50 μM) stoichiometry $(\alpha4)_3(\beta2)_2$ receptors. The maximal response is significantly reduced for the three lynx1 variants. There is no significant difference between lynx1, mCherry-lynx, and lynx1 plus PLC treatment. Numbers within parentheses in bar graphs represent number of cells per condition.

**Table 1.** Comparison of two-component fits to α4β2 dose-response relations in N2a cells when co-transfected with empty vector, or one of three lynx1 conditions

| **α4β2 ACh** | HS $EC_{50}$ | Err | HS n | Err | LS $EC_{50}$ | Err | LS n | Err | %HS | $R^2$ |
|---|---|---|---|---|---|---|---|---|---|---|
| wt +pcDNA | **2.34** | 1.38 | **0.86** | 0.43 | **36.9** | 20.1 | **1.5** | 0.76 | **50.3%** | **0.97** |
| +lynx-pTracer | **5.42** | 3.36 | **1.5** | 1.18 | **61.4** | 14.1 | **1.5** | 0.44 | **27.0%** | **0.99** |
| + mC-lynx | **2.49** | 1.41 | **1.05** | 0.76 | **58.6** | 12.8 | **1.5** | 0.37 | **28.4%** | **0.99** |
| Lynx+PLC | **6.55** | 9.47 | **0.54** | 0.41 | **41.9** | 14.7 | **1.5** | 0.37 | **24.9%** | **0.99** |

Table 1. Fitted parameters for ACh concentration-response relations of α4β2 when co-transfected with empty vector, lynx1-wt, mCherry-lynx1, and lynx1-wt after treatment with PI-PLC. Parameters correspond to ACh concentration-response relations in Figure 2-3. The $EC_{50}$ and Hill coefficient values represent the mean ± SEM for the number of measurements (n) obtained. The relative fraction of the high sensitivity component (1st comp) for the biphasic relations is included.lynx1, mCherry-lynx1, or lynx1 plus PLC treatment. Fits were generated under two assumptions: 1. All HS receptors, and no LS receptors, are activated at 10 μM ACh; 2. Hill coefficients were constrained to <= 1.5.

***PI-PLC treatment cleaves lynx1 from the plasma membrane***

We cleaved the GPI anchor of lynx1, releasing lynx1 from the PM via treatment with phosphatidylinositol-specific phospholipase C (PI-PLC). This allowed us to determine whether acute removal of surface lynx1 affects the response of α4β2 nAChRs. Using confocal imaging, we demonstrate that we can remove lynx1 from the PM of N2a cells expressing α4β2 nAChRs and mCherry-lynx1 (Figure 2-4). Before treatment with PI-PLC, "railroad tracks" of red fluorescence are clear on the borders of processes, indicating mCherry-lynx1 on the PM, and these are quantified by intensities in typical line profiles where the peaks align with the borders. After PI-PLC treatment for 1 h the membrane fluorescence is decreased and becomes undetectable above background (Figure 2-4A, B). This can be seen clearly through line profiles (Figure 2-4C, D). In control experiments,

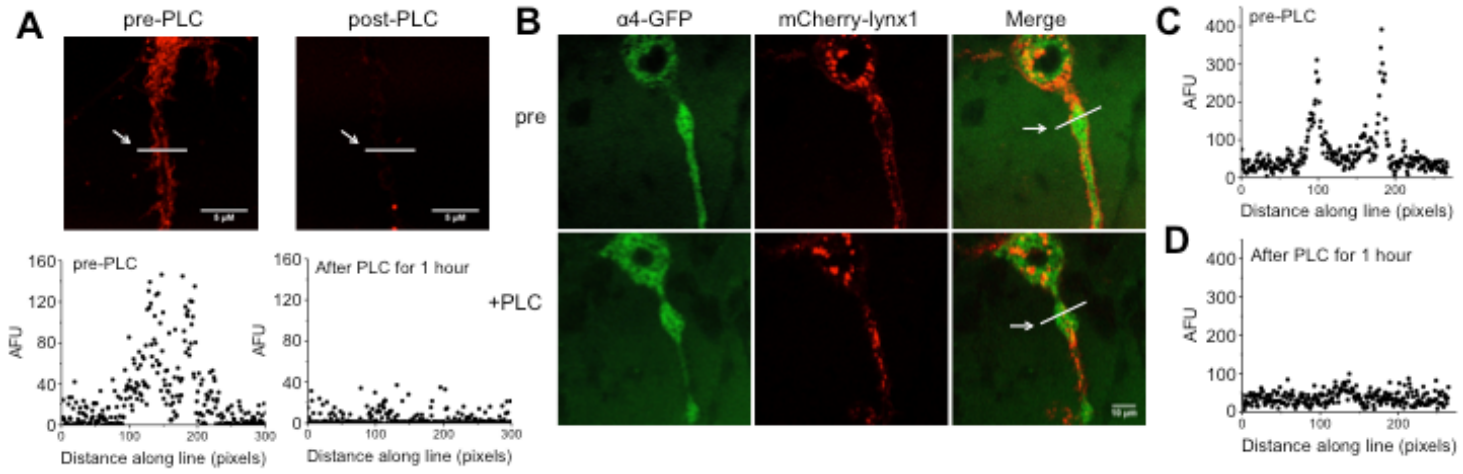


Figure 2-5. PI-PLC treatment cleaves mCherry-lynx1 from the plasma membrane. A, images of N2a cells transfected with α4-GFP, β2-wt, and mCherry-lynx1 taken with a confocal microscope before and after treatment with phosphatidylinositol-specific phospholipase C (PI-PLC). B-C, line profiles quantifying fluorescence levels across a line demonstrate the presence of the 'railroad track' morphology of mCherry-lynx1 on the membrane of N2a cells before treatment with PLC (B), and after (C). The arrows point to the lines used for quantification. 100 pixels = 10 μm. These data are typical of 5 experiments.

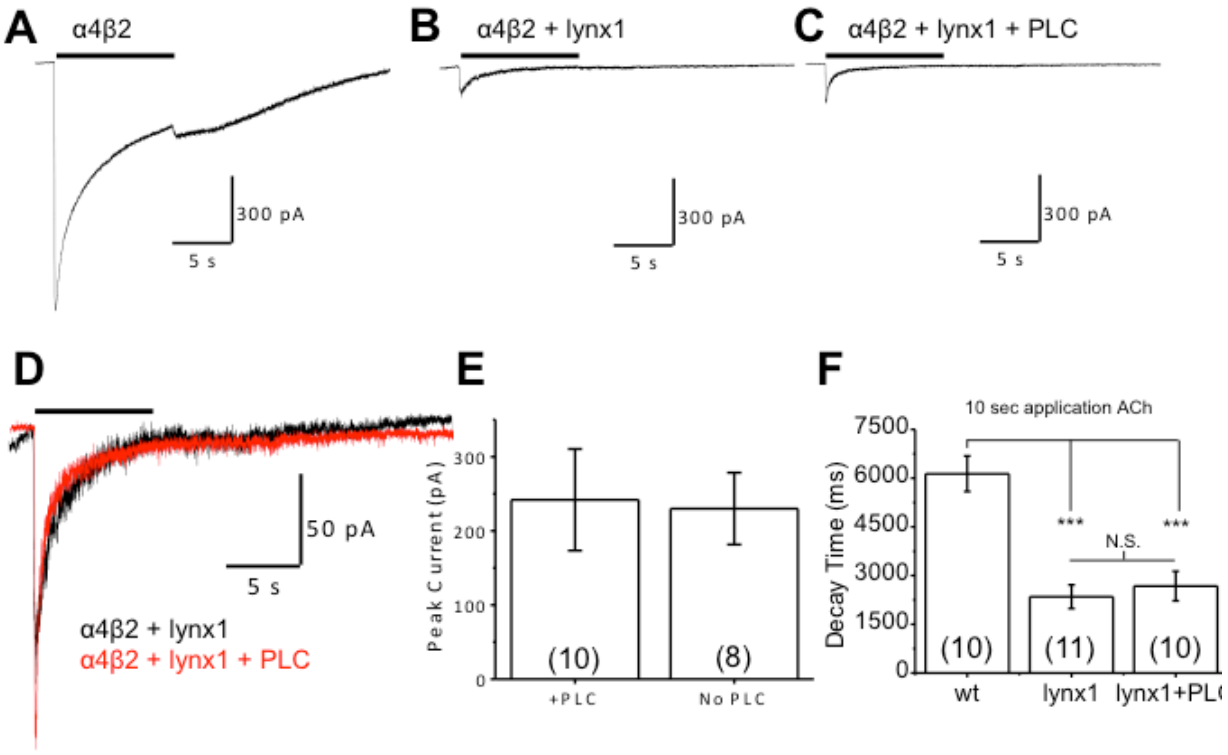


Figure 2-5. PLC treatment does not affect ACh-induced currents of cells transfected with α4β2 and lynx1. A-C, example traces from N2a cells transfected with α4, β2, and either (A) empty vector, (B) lynx1, or (C) lynx1 with subsequent PLC treatment. Cells were subjected to 100 μM ACh for 10 s to measure both peak current and desensitization (quantified here as the time between 90% and 10% of max current). D, Overlay of traces comparing lynx1 with or without PLC treatment. PLC does not alter peak current (E) or decay time (F) of N2a cells transfected with α4, β2, and lynx1. However, lynx1 does shorten the decay time compared to α4β2 alone both without and with PLC treatment. Panel F presents a shift in 90% to 10% decay time from 6.14 ± 0.55 sec for empty vector to 2.35 ± 0.37 sec and 2.68 ± 0.46 sec for lynx-wt and lynx1-wt + PLC, respectively

cells were treated with identical solution lacking PI-PLC and we observed no reduction in PM "railroad-track" appearance or line profile quantification (Figure 2-6).

***PI-PLC treatment does not affect dose response-relations to ACh, peak current, or signal decay time of α4β2 + lynx1.***

Before and after treatment with PI-PLC to cleave lynx1, we performed electrophysiological experiments to measure concentration-response relations to ACh (Figure 2-3F). After PI-PLC treatment, the peak currents and concentration response curve were not different when compared to lynx1-wt and mCherry-lynx1 conditions (Figure 2-3F). Peak current amplitude at saturating concentrations of ACh (300 μM) and desensitization kinetics (90% to 10% of maximal current) were not different when comparing lynx1-wt plus PLC and lynx1-wt without PI-PLC (Figure 2-5). We confirmed earlier observations that the presence of lynx does accelerate desensitization of α4β2 currents (Ibanez-Tallon et al., 2002; Miwa et al., 2006). However, this acceleration is not reversed by PI-PLC treatment. Overlay of α4β2 nAChRs with lynx1 (treated or not treated with PI-PLC) show a close overlap and little difference among waveforms (Figure 2-5D). These results suggest that the major effects of lynx1 on α4β2 occur before the nAChRs appear on the PM. The data together suggest that lynx1 exerts its effects intracellularly, stabilizing α4/α4 dimers in the ER, thus favoring the LS $(\alpha4)_3(\beta2)_2$ stoichiometry.

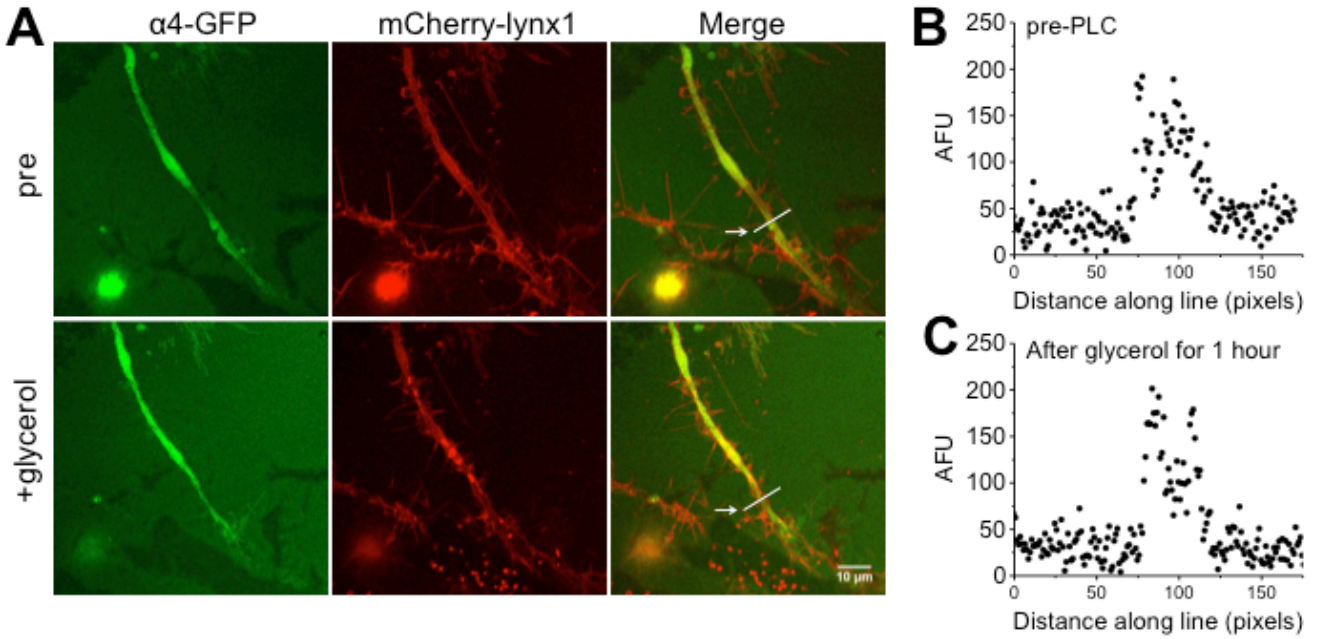


Figure 2-6. Control treatment does not affect the 'railroad track' fluorescence signal of mCherry-lynx1. A, images of N2a cells transfected with α4-GFP, β2, and mCherry-lynx1 before and after treatment with control glycerol-containing solution but without PLC. B-C, line profile quantifications visualize the persistence of the 'train-track' twin peaks as cells remain in an environment-controlled chamber on the confocal microscope.

# Discussion

Our data lead to three conclusions. First, we demonstrate that lynx1 binds α4 nAChR subunits in the ER and increases α4/α4 dimer formation. Second, lynx1 biases the stoichiometry of α4β2 receptors toward LS assembly of α4β2 nAChRs. Finally, the minimal effects of removing lynx1 at the PM suggest that lynx1 exerts its effects on nascent receptors within the ER, thereby influencing receptor assembly and the stoichiometry of the final receptor exported to the PM. To our knowledge, this is the first report of a GPI-anchored protein playing a role in regulating assembly of a multimeric protein through an intracellular mechanism.

It has been previously demonstrated that the expression of lynx1 shifts α4β2 to the LS stoichiometry, and the removal of lynx1 increases sensitivity (Ibanez-Tallon et al., 2002; Miwa et al., 2006). The molecular mechanisms for these actions, however, had yet to be addressed. Taking into account the relationship between lynx genes and snake venom toxins, a straightforward mechanism of lynx binding to the extracellular portion of the receptor on the cell surface to influence gating, has been the assumed mode of action for lynx proteins (Lyukmanova et al., 2011; Miwa et al., 1999). In this study, we applied new tools to demonstrate that lynx1 is resident both on the cell surface and in the interior of the cell. Apparently, the internal lynx1/α4 interactions are dominant, because removing surface lynx had little effect on receptor function. The most likely mechanism is that lynx1 controls the functional properties of nAChRs by influencing the type and number of receptors during receptor assembly.

If lynx1 does exert a functional gating effect on PM α4β2 nAChRs, it may be effective after cleavage of the GPI anchor and/or at very high concentrations. Indeed,

exogenously applied lynx1 (minus the GPI anchor) alters the peak response of α4β2 nAChRs to nicotine and ACh *in vitro* (Miwa et al., 1999). Further, previous studies *in vivo* show that overexpression of secreted lynx1 in mouse cerebellum, a region involved in motor learning, results in enhanced motor learning (Miwa and Walz, 2012), a behavioral phenotype similar to the lynx1-KO mice. Our results cannot definitively exclude a mechanism by which the lynx1 proteins that were previously bound to receptors prior to PI-PLC treatment remained bound after GPI-anchor cleavage. In this scenario, these interactions may have continued to influence gating function, but the concentration of bound lynx molecules were below the detection threshold of our confocal imaging assay. A mechanism in which the normal function of lynx1 is to act in trans at the post-synaptic membrane was not addressed and awaits further studies.

Single channel studies of α4β2 and lynx1 in CHO cells indicate a shift in the proportion of channel openings toward higher amplitude, faster inactivating species (Ibanez-Tallon et al., 2002). The two different amplitudes of single channel openings may arise from the two different stoichiometries, where the $(\alpha4)_3(\beta2)_2$ stoichiometry mediates larger amplitude opening (Tapia et al., 2007). The interactions of lynx1 and α4/ α4 subunits are likely to shift the internal concentration of total α4/α4 interfaces, and since an α4/α4 interface occurs only in the $(\alpha4)_3(\beta2)_2$ nAChR stoichiometry, then this could explain the greater expression of $(\alpha4)_3(\beta2)_2$ nAChRs when lynx1 is present. Since $(\alpha4)_3(\beta2)_2$ nAChRs are also thought to inactivate more rapidly. The accelerated decay of the macroscopic current in cells co-transfected with lynx1 might be explained by this stoichiometry shift. A lynx1 based model of pentameric receptor assembly might be slightly different than those previously put forth. It is generally thought that α4/β2 dimers are formed first, and the fifth

position is filled by either an α4 or β2 subunit. The lynx1-nAChR interaction might affect this final step, in favor of incorporating α4 subunits. Increasing the α4/α4 population may influence the expression of fully formed receptors, resulting in both greater selectivity (shift in stoichiometry), and less efficiency (reduction in the total number of receptors).

The preferential affinity of lynx1 for α/α interfaces invites parallels with the ability of α-Btx to bind to α7 nAChRs. We might predict that the effect of lynx1 on monomeric nAChRs would differ from effects on those that can express multiple stoichiometries. It is interesting to note that nicotine binds to α/β interfaces, and prolonged nicotine binding within the ER is thought to upregulate α4β2 nAChRs by stabilizing the $(\alpha4)_2(\beta2)_3$ stoichiometry (Henderson et al., 2014; Lester et al., 2009; Nashmi et al., 2007; Srinivasan et al., 2011). Our data suggest that lynx1 could oppose some of the effects of chronic nicotine, by shifting the dimer concentration towards the α4/α4 species (Ibanez-Tallon et al., 2002). The differential up-regulation by chronic nicotine exposure in the brain may be due in part to the differential expression of lynx1 genes in different neuronal cell types.

Our data are consistent with the possibility that interactions between α4 nAChR subunits and lynx1 could be a long-term interaction initiated in the ER, and sustained throughout the lifetime of the receptor. This presents the possibility of a multi-modal action of lynx1 on several aspects of cholinergic signaling. This should be taken into account when one considers models of lynx1 action on the function of the cholinergic system in the brain. The control that lynx1 exerts on cholinergic tone through nAChR interactions (Miwa et al., 2011; Miwa et al., 2012; Morishita et al., 2010), makes lynx1 a reasonable target for pharmaceutical drug development. There are several drug candidates targeting nAChRs in development (Gault et al., 2013; Hauser et al., 2009; Lieberman et al., 2013; Prickaerts et

al., 2012), and some may act by potentiating nAChRs (Harvey et al., 2014; Kanner, 2013; Prickaerts et al., 2012; Putman and Dasse, 2013; Timmermann et al., 2007). One potential drawback of strategies involving agonists or partial agonists is the uncertainty of either receptor activation or desensitization, or both (Buisson and Bertrand, 2001; Lester et al., 2004). The lynx family proteins appear to increase the rate of desensitization of nAChRs (Ibanez-Tallon et al., 2004; Tekinay et al., 2009), and their removal results in nAChRs exhibiting less receptor desensitization. Therefore, inhibition of the endogenous action of lynx proteins may achieve the possibly desirable effect of increasing cholinergic tone while reducing desensitization. The majority of attention in pharmaceutical development is directed towards actions of compounds acting on receptors on the PM. Our data suggest that it may be important to consider intracellular mechanisms of action as well.

# References

Buisson B, and Bertrand D (2001) Chronic exposure to nicotine upregulates the human a4b2 nicotinic acetylcholine receptor function. J Neurosci 21:1819-29.

Chimienti F, Hogg RC, Plantard L, Lehmann C, Brakch N, Fischer J, Huber M, Bertrand D, and Hohl D (2003) Identification of SLURP-1 as an epidermal neuromodulator explains the clinical phenotype of Mal de Meleda. Hum Mol Genet 12:3017-24.

Drenan RM, Nashmi R, Imoukhuede PI, Just H, McKinney S, and Lester HA (2008) Subcellular Trafficking, Pentameric Assembly and Subunit Stoichiometry of Neuronal Nicotinic ACh Receptors Containing Fluorescently-Labeled α6 and β3 Subunits. Mol Pharmacol 73:27-41.

Gault L, Ritchie C, Robieson W, Pritchett Y, Othman A, and Lenz R (2013) Efficacy and safety of the alpha7 agonist ABT-126 in mild-to-moderate Alzheimer's dementia. Alzheimer's & Dementia: The Journal of the Alzheimer's Association 9:P138-P138.

Gotti C, Clementi F, Fornari A, Gaimarri A, Guiducci S, Manfredi I, Moretti M, Pedrazzi P, Pucci L, and Zoli M (2009) Structural and functional diversity of native brain neuronal nicotinic receptors. Biochemical pharmacology 78:703-711.

Harvey A, Fluck A, Giethlen B, Paul D, and Schaeffer L (2014) Positive Allosteric Modulators of the Alpha 7 Nicotinic Acetylcholine Receptor and uses Thereof: US Patent Application 13/983,476.

Hauser TA, Kucinski A, Jordan KG, Gatto GJ, Wersinger SR, Hesse RA, Stachowiak EK, Stachowiak MK, Papke RL, Lippiello PM, and Bencherif M (2009) TC-5619: An alpha7 neuronal nicotinic receptor-selective agonist that demonstrates efficacy in animal models of the positive and negative symptoms and cognitive dysfunction of schizophrenia. Biochemical pharmacology 78:803-812.

Henderson BJ, Srinivasan R, Nichols WA, Dilworth CN, Gutierrez DF, Mackey ED, McKinney S, Drenan RM, Richards CI, and Lester HA (2014) Nicotine exploits a COPI-mediated process for chaperone-mediated up-regulation of its receptors. J Gen Physiol 143:51-66.

Ibanez-Tallon I, Miwa JM, Wang HL, Adams NC, Crabtree GW, Sine SM, and Heintz N (2002) Novel modulation of neuronal nicotinic acetylcholine receptors by association with the endogenous prototoxin lynx1. Neuron 33:893-903.

Ibanez-Tallon I, Wen H, Miwa JM, Xing J, Tekinay AB, Ono F, Brehm P, and Heintz N (2004) Tethering naturally occurring peptide toxins for cell-autonomous modulation of ion channels and receptors in vivo. Neuron 43:305-11.

Jacob TC, Bogdanov YD, Magnus C, Saliba RS, Kittler JT, Haydon PG, and Moss SJ (2005) Gephyrin regulates the cell surface dynamics of synaptic $GABA_A$ receptors. Journal of Neuroscience 25:10469-10478.

Jensen AA, Frolund B, Liljefors T, and Krogsgaard-Larsen P (2005) Neuronal nicotinic acetylcholine receptors: structural revelations, target identifications, and therapeutic inspirations. J Med Chem 48:4705-45.

Kanner R (2013) α-7 nicotinic acetylcholine receptor allosteric modulators, their derivatives and uses thereof: US Patent 8,563,579.

Kenworthy AK (2004) Dynamics of putative raft-associated proteins at the cell surface. The Journal of Cell Biology 165:735-746.

Khiroug SS, Pryazhnikov E, Coleman SK, Jeromin A, Keinanen K, and Khiroug L (2009) Dynamic visualization of membrane-inserted fraction of pHluorin-tagged channels using repetitive acidification technique. BMC Neuroscience 10.

Lester H, Dibas M, Dahan DS, Leite JF, and Dougherty DA (2004) Cys-loop receptors: new twists and turns. Trends Neurosci 27:329-336.

Lester HA, Xiao C, Srinivasan R, Son C, Miwa J, Pantoja R, Dougherty DA, Banghart MR, Goate AM, and Wang JC (2009) Nicotine is a Selective Pharmacological Chaperone of Acetylcholine Receptor Number and Stoichiometry. Implications for Drug Discovery. AAPS Journal 11:167-77.

Lieberman JA, Dunbar G, Segreti AC, Girgis RR, Seoane F, Beaver JS, Duan NH, and Hosford DA (2013) A Randomized Exploratory Trial of an Alpha-7 Nicotinic Receptor Agonist (TC-5619) for Cognitive Enhancement in Schizophrenia. Neuropsychopharmacology 38:968-975.

Lyukmanova EN, Shenkarev ZO, Shulepko MA, Mineev KS, D'Hoedt D, Kasheverov IE, Filkin SY, Krivolapova AP, Janickova H, Dolezal V, Dolgikh DA, Arseniev AS, Bertrand D, Tsetlin VI, and Kirpichnikov MP (2011) NMR structure and action on nicotinic acetylcholine receptors of water-soluble domain of human lynx1. J Biol Chem.

Miesenböck G, De Angelis DA, and Rothman JE (1998) Visualizing secretion and synaptic transmission with pH-sensitive green fluorescent proteins. Nature 394:192-195.

Miwa JM, Freedman R, and Lester HA (2011) Neural systems governed by nicotinic acetylcholine receptors: emerging hypotheses. Neuron 70:20-33.

Miwa JM, Ibanez-Tallon I, Crabtree GW, Sanchez R, Sali A, Role LW, and Heintz N (1999) lynx1, an endogenous toxin-like modulator of nicotinic acetylcholine receptors in the mammalian CNS. Neuron 23:105-14.

Miwa JM, Lester HA, and Walz A (2012) Optimizing cholinergic tone through lynx modulators of nicotinic receptors: implications for plasticity and nicotine addiction. Physiology 27:187-99.

Miwa JM, Stevens TR, King SL, Caldarone BJ, Ibanez-Tallon I, Xiao C, Fitzsimonds RM, Pavlides C, Lester HA, Picciotto MR, and Heintz N (2006) The Prototoxin lynx1 Acts on Nicotinic Acetylcholine Receptors to Balance Neuronal Activity and Survival In Vivo. Neuron 51:587-600.

Miwa JM, and Walz A (2012) Enhancement in motor learning through genetic manipulation of the Lynx1 gene. PloS one 7:e43302.

Morishita H, Miwa J, Heintz N, and Hensch T (2010) Lynx1, a cholinergic brake, limits plasticity in adult visual cortex. Science 330:1238-1240.

Moroni M, Zwart R, Sher E, Cassels BK, and Bermudez I (2006) α4β2 nicotinic receptors with high and low acetylcholine sensitivity: pharmacology, stoichiometry, and sensitivity to long-term exposure to nicotine. Mol Pharmacol 70:755-68.

Moss FJ, Imoukhuede PI, Scott K, Hu J, Jankowsky JL, Quick MW, and Lester HA (2009) GABA transporter function, oligomerization state, and anchoring: correlates with subcellularly resolved FRET. J Gen Physiol 134:489-521.

Nashmi R, Dickinson ME, McKinney S, Jareb M, Labarca C, Fraser SE, and Lester HA (2003) Assembly of a4b2 nicotinic acetylcholine receptors assessed with functional fluorescently labeled subunits: effects of localization, trafficking, and nicotine-induced upregulation in clonal mammalian cells and in cultured midbrain neurons. J Neurosci 23:11554-67.

Nashmi R, Xiao C, Deshpande P, McKinney S, Grady SR, Whiteaker P, Huang Q, McClure-Begley T, Lindstrom JM, Labarca C, Collins AC, Marks MJ, and Lester HA (2007) Chronic nicotine cell specifically upregulates functional α4* nicotinic receptors: basis for both tolerance in midbrain and enhanced long-term potentiation in perforant path. J Neurosci 27:8202-18.

Nelson ME, Kuryatov A, Choi CH, Zhou Y, and Lindstrom J (2003) Alternate stoichiometries of a4b2 nicotinic acetylcholine receptors. Mol Pharmacol 63:332-41.

Nichols BJ, Kenworthy AK, Polishchuk RS, Lodge R, Roberts TH, Hirschberg K, Phair RD, and Lippincott-Schwartz J (2001) Rapid cycling of lipid raft markers between the cell surface and Golgi complex. The Journal of Cell Biology 153:529-541.

Prickaerts J, van Goethem NP, Chesworth R, Shapiro G, Boess FG, Methfessel C, Reneerkens OAH, Flood DG, Hilt D, Gawryl M, Bertrand S, Bertrand D, and König G

(2012) EVP-6124, a novel and selective α7 nicotinic acetylcholine receptor partial agonist, improves memory performance by potentiating the acetylcholine response of α7 nicotinic acetylcholine receptors. Neuropharmacology 62:1099-1110.

Putman D, and Dasse O (2013) Alpha 7 nicotinic acetylcholine receptor allosteric modulators, their derivatives and uses thereof: Patent Application PCT WO-13169889.

Richards CI, Srinivasan R, Xiao C, Mackey ED, Miwa JM, and Lester HA (2011) Trafficking of α4* nicotinic receptors revealed by superecliptic phluorin: effects of a β4 amyotrophic lateral sclerosis-associated mutation and chronic exposure to nicotine. J Biol Chem 286:31241-9.

Srinivasan R, Henderson BJ, Lester HA, and Richards CI (2014) Pharmacological chaperoning of nAChRs: A therapeutic target for Parkinson's disease. Pharmacological Research.

Srinivasan R, Pantoja R, Moss FJ, Mackey EDW, Son C, Miwa J, and Lester HA (2011) Nicotine upregulates α4β2 nicotinic receptors and ER exit sites via stoichiometry-dependent chaperoning. J Gen Physiol 137:59-79.

Tapia L, Kuryatov A, and Lindstrom J (2007) $Ca^{2+}$ permeability of the $(\alpha4)_3(\beta2)_2$ stoichiometry greatly exceeds that of $(\alpha4)_2(\beta2)_3$ human acetylcholine receptors. Mol Pharmacol 71:769-76.

Tekinay AB, Nong Y, Miwa JM, Lieberam I, Ibanez-Tallon I, Greengard P, and Heintz N (2009) A role for LYNX2 in anxiety-related behavior. Proc Natl Acad Sci U S A 106:4477-82.

Timmermann DB, Grønlien JH, Kohlhaas KL, Nielsen EØ, Dam E, Jørgensen TD, Ahring PK, Peters D, Holst D, and Chrsitensen JK (2007) An allosteric modulator of the α7 nicotinic acetylcholine receptor possessing cognition-enhancing properties in vivo. Journal of Pharmacology and Experimental Therapeutics 323:294-307.

Whiteaker P, Sharples CG, and Wonnacott S (1998) Agonist-induced up-regulation of a4b2 nicotinic acetylcholine receptors in M10 cells: pharmacological and spatial definition. Mol Pharmacol 53:950-62.

# Chapter III:
# The β2V287L mutation suppresses formation of the lower sensitivity stoichiometry of α4β2 and increases α5α4β2 on the plasma membrane*

*This chapter will be submitted as a manuscript to Molecular Pharmacology by the authors Weston A. Nichols, Brandon J. Henderson, Caroline Y. Yu, Chris B. Marotta, Christopher I. Richards, Bruce N. Cohen, and Henry A. Lester.

# Abstract

A number of mutations in α4β2-containing (α4β2*) nicotinic acetylcholine (ACh) receptors (nAChRs) are linked to autosomal dominant nocturnal frontal lobe epilepsy (ADNFLE). Several increase the sensitivity, and reduce allosteric $Ca^{2+}$ potentiation, of the α4β2 ACh response. Two α4β2 subtypes, with different subunit stoichiometries $(\alpha4)_2(\beta2)_3$ and $(\alpha4)_3(\beta2)_2$, exist in the cortex, along with α5α4β2 nAChRs. Previous results suggest that a knock-in mouse bearing the ADNFLE mutation β2V287L displays little functional expression of the $(\alpha4)_3(\beta2)_2$ subtype. However, this hypothesis has not been tested using heterologously expressed receptors. We measured the effects of the β2V287L mutation on α4β2 and α5α4β2 nAChRs expressed in oocytes and mammalian cell lines using electrophysiological techniques, a voltage-sensitive fluorescent dye, and TIRF imaging of superecliptic pHlourin (SEP) tagged constructs. In oocytes, β2V287L reduced $EC_{50}$ values for the high-senstitivity, $(\alpha4)_2(\beta2)_3$, and low-sensitivity, $(\alpha4)_3(\beta2)_2$, nAChRs by a similar factor and suppressed functional, low-sensitivity receptor plasma membrane (PM) expression. However, it did not affect the $EC_{50}$ of α5α4β2 nAChRs. In mammalian cells, measurements of the α4β2 ACh response using a voltage-sensitive fluorescent dye and whole-cell patch-clamping demonstrated that while β2V287L reduced the overall α4β2 maximum response, it increased the α4β2 response to sub-saturating ACh (1-10 μM). Imaging of SEP-tagged α5, α4, β2, and β2V287L subunits demonstrated that β2V287L reduced total α4β2 nAChR PM expression, increased the mean number of β2 subunits per α4β2 nAChR on the PM, and increased the surface expression of α5* nAChRs. Thus, mutations linked to ADNFLE can have subtype-selective effects on α4β2 nAChRs.

# Introduction

Autosomal dominant nocturnal frontal lobe epilepsy (ADNFLE) is an inherited partial epilepsy linked to mutations in α2, α4, and β2 nicotinic acetylcholine (ACh) receptor (nAChR) subunits. Recent studies also link ADNFLE to mutations in a sodium-gated potassium channel *KCNT1* (Heron et al., 2012) and, possibly, the corticotrophin releasing hormone (CRH) (Sansoni et al., 2013). ADNFLE patients display brief nocturnal seizures that occur primarily during slow-wave (SW) sleep and originate in the frontal lobe. Penetrance for the nicotinic ADNFLE mutations ranges from 29% to 100% (Ferini-Strambi et al., 2012). Patient seizures typically begin between five and fifteen years of age (Scheffer et al., 1995). This time frame coincides with a developmental shift in the focus of slow-wave activity during sleep from the posterior brain to the frontal lobe (Kurth et al., 2010). The resulting increase in synchronized firing in the frontal lobe during SW sleep may facilitate the onset of ADNFLE seizures at this particular developmental stage. The pathophysiology of ADNFLE is not understood. However, a number of the nicotinic mutations linked to ADNFLE increase the sensitivity of α4β2 nAChRs to the endogenous agonist ACh and reduce $Ca^{2+}$ potentiation of the ACh response.

The β2V287L mutation is one of several nicotinic mutations linked to ADNFLE. Nicotinic receptors consist of five subunits arranged around a central pore. The β2V287L mutation is located near the extracellular entrance to the narrow part of the pore at the 22' position (where position 1' is the amino-terminus of the M2 transmembrane domain). This mutation produces several changes in the functional properties of heterologously expressed α4β2 nAChRs, including a reduction in the apparent rate of agonist-induced

desensitization, an increase in agonist-induced steady-state desensitization, a reduction in single-channel conductance, an increase in ACh sensitivity, and a reduction in $Ca^{2+}$ potentiation of the ACh response (De Fusco et al., 2000; Rodrigues-Pinguet et al., 2003, 2005). Electroencephalographic (EEG) recordings from transgenic mice with untargeted β2V287L transgene insertions show that the mice display epileptiform activity during bouts of increased delta activity (presumably corresponding to SW sleep). Silencing conditionally-expressed mutant β2V287L transgenes in adult mice does not prevent epileptiform activity, but silencing it during early development does, even though the mutant transgene is later expressed in the adult mouse. Thus, the developmental effects of the β2V287L mutation appear to be a key feature of ADNFLE epileptogenesis (Manfredi et al., 2009).

Knock-in mice with targeted β2V287L insertions display increased mortality (possibly because of unobserved epileptic seizures) and behavioral abnormalities but apparently not spontaneous epileptiform EEG activity. The behavioral abnormalities of these mice include reduced nocturnal running wheel activity, increased ambulatory activity, increased locomotor habituation, and decreased anxiety-related behavior (Xu et al., 2011). The mice also display altered nicotine-induced behaviors such as an increased sensitivity to nicotine-induced seizure signs, novel nicotine-induced tonic forelimb and digit extension, enhanced sensitivity to nicotine-induced hypothermia, and enhanced sensitivity to nicotine-induced Y-maze behaviors. The β2V287L mutation affects both the function and expression of α4β2* nAChRs *in situ* (O'Neill et al., 2013). The mutation significantly reduces the overall amount of α4β2* nAChR protein (but not mRNA) expressed in the brain (as measured by cytisine-sensitive [$^{125}$I]epibatidine and mAb270 binding), reduces

maximal ACh-induced $^{86}$Rb, [$^{3}$H]dopamine (DA), and cortical [$^{3}$H]GABA release from mouse brain synaptosomes (O'Neill et al., 2013), and increases the sensitivity of ACh-induced $^{86}$Rb, [$^{3}$H]dopamine (DA), and [$^{3}$H]GABA synaptosomal release.

The α4 and β2 nicotinic subunits are capable of forming functional α4β2 pentameric receptors with different subunit stoichiometries in heterologous expression systems (Zwart and Vijverberg, 1998). The two most common stoichiometries are $(\alpha4)_2(\beta2)_3$ and $(\alpha4)_3(\beta2)_2$. The ACh sensitivity of $(\alpha4)_2(\beta2)_3$ receptors is ~100 times higher than that of $(\alpha4)_3(\beta2)_2$ receptors (Moroni et al., 2006). Consistent with these data, the ACh concentration-response relations for α4β2*-mediated $^{86}$Rb synaptosomal efflux is biphasic (Gotti et al., 2008). Thus, both native α4β2* nAChRs as well as heterologously expressed α4β2 nAChRs appear to be capable of assembling into functional receptors with two alternate α4:β2 stoichiometries. Studies of mice with partial α4 and β2 gene deletions suggest that $(\alpha4)_2(\beta2)_3$ receptors mediate high-sensitivity (HS) ACh-induced $^{86}$Rb release from cortical and thalamic synaptosomes, and $(\alpha4)_3(\beta2)_2$ receptors mediate LS release (Gotti et al., 2008).

In the knock-in mouse model, the β2V287L mutation significantly reduces the LS component of the ACh concentration-response relation for $^{86}$Rb efflux from cortical synaptosomes but does not significantly affect the amplitude of the HS component (O'Neill et al., 2013). Selective suppression of the LS component suggests that the β2V287L mutation may inhibit formation of the LS $(\alpha4)_3(\beta2)_2$ expression. Selective LS suppression may also account for some previously reported effects of the ADNFLE mutations on the ACh concentration-response relation. However, the sole previous study of how ADNFLE mutations affect subunit stoichiometry of α4β2 nAChRs suggests that they,

in fact, increase the fraction of $(\alpha4)_3(\beta2)_2$ (LS) receptors in the population (Son et al., 2009).

We used two approaches to determine whether the β2V287L mutation affects the subunit stoichiometry, and ACh sensitivity, of α4β2 nAChRs expressed in oocytes and mammalian cell lines. The first approach was to bias HS and LS α4β2 expression by systematically varying ratio of α4:β2 cRNA injected into oocytes and measure the effects of the mutation on the ACh concentration-response relations of the expressed receptors. We also studied the effects of the mutation on α4β2 nAChRs expressed in mammalian cell lines using a fluorescent membrane potential assay and whole-cell patch clamp electrophysiology. The second approach was to tag α4, β2, α5, and β2V287L subunits with superecliptic pHlourin (SEP) and measure the effects of the mutation on expression of the tagged subunits in the endoplasmic reticulum (ER) and plasma membrane (PM) of a mammalian cell line (Miesenbock et al., 1998). SEP is a pH-sensitive GFP analog that in fluorescent at in basic conditions, but quenched in acidic solution, with a pKa ~7.0. Perfusing cells with acidic extracellular solution quenches fluorescent PM proteins with extracellular SEP tags. Thus, surface α4-, β2-, and β2V287L-SEP subunit expression can be estimated by measuring the acid-induced reduction in total subunit fluorescence (Richards et al., 2011).

The α5 nicotinic subunit co-assembles with α4 and β2 to form a high-sensitivity α5α4β2 nAChR (Brown et al., 2007). To determine whether the β2V287L mutation alters the expression, and/or ACh sensitivity, of α5α4β2 nAChRs, we measured the effects of the mutation on the ACh concentration-response relations of α4β2 and α5α4β2 nAChRs expressed in both oocytes and mammalian cells, and on α5α4β2 surface expression using

SEP-tagged α5 subunits (α5-SEP). The results show that β2V287L increases the ACh sensitivity of both HS and LS α4β2 nAChRs, inhibits the formation of LS α4β2 nAChRs, and enhances α5α4β2 nAChR surface expression without affecting α5α4β2 ACh sensitivity.

# Experimental Procedures

### *Molecular Biology*

For mammalian cell expression, we used wild-type (WT) mouse α4, α5, and β2 cDNA clones inserted into pCI-NEO vectors. To measure subunit expression in the PM, C-terminal superecliptic pHluorin (SEP) tags were added to the α5 and β2 subunits using a previously described PCR protocol and primers that overlapped the C-terminals of the coding sequences (Richards et al., 2011). The forward primer for the α5-SEP reaction was 5'-ACATTGGAAACACAATTAAGATGAGTAAAGGAGAAGAACT-3', and the reverse primer was 5'-CGGGCCCTCTAGATCNTCAGGTTATTTGTATAGTTCATCCA -3'. The forward primer for the β2-SEP reaction was 5′-ACTCAGCTCCCAGCTCCAAGATGAGTAAAGGAGAAGAACT-3′ and the reverse primer was 5′- GGAGCTGCAAATGAGAGACCTTATTTGTATAGTTCATCCA-3′. After reaction completion, the resulting PCR products were cloned into a vector containing either the α5 or β2 cDNA clone using Pfu-Turbo polymerase. The mouse α4-SEP was constructed previously using the same protocol (Richards et al.). We used the QuikChange II XL site-directed mutagenesis kit with the forward primer 5′-CTGCTCATCTCCAAGATTCTGCCTCCCACCTCCCTCGACGTA-3′ and the reverse primer 5′-TACGTCGAGGGAGGTGGGAGGCAGAATCTTGGAGATGAGCAG-3′ to construct the β2V287L mutation. For oocyte expression, we used mouse nAChR α5, α4 and β2 cDNA clones inserted into pGEMHE vectors. The QuikChange protocol (Stratagene) was used for site-directed mutagenesis. To make cRNAs for the oocyte injections, α4 and β2 cDNA plasmids were linearized using *SbfI*. The α5 plasmid was

linearized using *SphI*. Linearized DNA was purified (Qiagen) and cRNA was synthesized from it using the T7 mMessage Machine kit (Ambion). The Qiagen RNeasy RNA purification kit was used to purify synthesized cRNA.

***Tissue Culture and Transfection***

Mouse Neuro-2a (N2a) cells were cultured using standard techniques and maintained in DMEM supplemented with 10% FBS. N2a cells were plated by adding 90,000 cells to poly-d-lysine-coated 35-mm glass-bottom imaging dishes (MatTek Corp.). The day after plating, plasmid DNA was mixed with cationic lipids by adding 500-750 ng of each nAChR plasmid to 4 μl of Lipofectamine 2000 transfection reagent in 200 μl of DMEM. After 20 min at ambient temperature, the transfection mixture was added to N2a cells in 1 ml of plating medium and incubated at 37 °C for 24 h. Dishes were rinsed twice with plating medium and incubated at 37 °C for another 24 h before imaging or performing electrophysiological experiments.

HEK cells were also cultured using standard cell techniques as detailed above. The cells were plated onto black-bottom 96-well plates at a density of 50,000 cells per well. The next day, they were transfected with 100 ng of the appropriate cDNA mixtures combined with 4 uL of Lipofectamine 2000, as described above. Transfected cells were used 24 h later for the fluorescent membrane potential assay.

***Fluorescent Membrane Potential Assay***

We used a fluorescent plate reader (FlexStation III, Molecular Devices, Sunnyvale, CA) and a proprietary voltage-sensitive dye to measure the ACh concentration-response

relations of nAChRs expressed in HEK cells. The cells were transiently transfected with nAChR subunits and plated in flat-bottom 96-well plates. One day after plating, ACh voltage responses were measured visually using the Membrane Potential Blue-Dye Kit (Molecular Devices, Sunnyvale, CA). ACh was added to the wells at a speed of 16 mL/sec. The peak response was used to construct the ACh concentration-response relations.

***Oocyte Injections and Electrophysiology***

We used a standard protocol approved by the Office of Laboratory Animal Research at the California Institute of Technology to surgically harvest *Xenopus laevis* stage V and VI oocytes. To express α4α5β2 nAChRs in the oocytes, α5, α4 and β2 mRNAs were mixed in a ratio of 10:1:1 (*w*/*w*/*w*) to produce a final concentration of 0.8 ng/nL. Individual oocytes were then injected with 50 nL of this mixture, to deliver a total of 40 ng of mRNA per oocyte. To express α4β2 nAChRs, α4 and β2 mRNAs were mixed in a ratio of 1:1 or 10:1 to produce final concentrations of 0.13 ng/nL or 0.42 ng/nL, respectively. The oocytes were injected with a total of 6.7 ng or 21 ng of mRNA, respectively (in 50 nL). After injection, the oocytes were incubated in ND96+ medium (96 mM NaCl, 2 mM KCl, 1.8 mM $CaCl_2$, 1.8 mM $MgCl_2$, 5 mM HEPES, 2.5 mM Na pyruvate, 0.6 mM theophylline, 50 mg/mL gentamycin, 5% horse serum, pH 7.4) at 18° C for 24-96 h. Acetylcholine chloride was purchased from Sigma-Aldrich and dissolved in a nominally $Ca^{2+}$-free ND96 buffer (96 mM NaCl, 2 mM KCl, 1 mM $MgCl_2$, 5 mM HEPES at pH 7.5). An automated two-electrode voltage-clamp (OpusXpress 6000A, Axon Instruments) was used to record ACh-induced currents from the injected oocytes at a holding potential of -60 mV. $Ca^{2+}$-free ND96 was used as the recording saline. To measure the ACh response, ACh was

microperfused onto the oocytes for 15 seconds followed by a 2 min saline rinse. To generate the ACh concentration-response relations, we applied 18 different concentrations of ACh to a single oocyte. Data were low-passed filtered at 5 Hz prior and sampled digitally at 20 Hz.

***Whole-Cell Patch Clamping***

N2a cells were co-transfected with nicotinic subunits and GFP to facilitate visual identification of cells expressing nicotinic receptors. We used an inverted fluorescence microscope (IX71, Olympus) equipped with a high-pressure Hg lamp (HB-10103AF, Nikon) to visualize fluorescing cells. Whole-cell voltage-clamp currents were recorded using an Axopatch-1D amplifier (Axon Instruments) and digitized with a Digidata 1440A analog-to-digital converter (Axon Instruments) under the control of the pClamp 10.0 software (Axon Instruments). The pipette-filling solution contained (in mM): 135 K gluconate, 5 KCl, 5 EGTA, 0.5 $CaCl_2$, 10 HEPES, 2 Mg-ATP, and 0.1 GTP (pH was adjusted to 7.2 with Tris-base, osmolarity to 280-300 mOsm with sucrose). Patch electrode input resistance was 2-4 MΩ. All recordings were obtained at ambient temperature. The data were low-passed filtered at 2 kHz and sampled at 10 kHz. ACh was dissolved in an extracellular solution containing (in mM): 140 NaCl, 5 KCl, 2 $CaCl_2$, 1 $MgCl_2$, 10 HEPES, and 10 glucose (320 mOsm, pH to 7.3 with Tris-base), and microperfused onto cells using either pressure ejection through a glass micropipette (0.3 s pulse of 20 psi) or a commercially available microperfusion system (Octaflow II, ALA Scientific Instruments). The holding potential was -50 mV. To minimize agonist-induced desensitization, we

applied ACh at 3 min intervals, and continually perfused the recording chamber with saline.

***TIRF Microscopy***

Live N2a cells were imaged 24 h after transfection in a stage-mounted culture dish incubator at 37 °C (Warner Instruments). Total internal reflection fluorescence microscopy (TIRFM) allowed us to visualize fluorescently labeled intracellular molecules within 200 nm of the cell-coverslip interface. TIRF images were obtained using an inverted microscope (IX81; Olympus) equipped with an Olympus PlanApo 100× 1.45 NA oil objective and a stepper motor (Thorlabs) to control the position of the fiber optic and TIRF evanescent field illumination. The microscope included a drift control module that maintained samples at a constant focus for periods of ≥24 h. Neuronal medium was exchanged for a simpler extracellular solution (ECS) (in mM: 150 NaCl, 4 KCl, 10 HEPES, 2 $MgCl_2$, 2 $CaCl_2$, and 10 glucose, pH 5.4 or 7.4) prior to imaging. SEP was excited using the 488-nm line of a multiline air-cooled argon laser (IMA101040ALS; Melles Griot). Images were captured with a back-illuminated EMCCD camera (iXON DU-897). Frame rates, laser power settings, and camera gain parameters were initially adjusted and maintained at a constant setting across all samples for each imaging session. We acidified the imaging dish by perfusing the bath (normally pH 7.4) with an otherwise identical solution adjusted to pH 5.4. The ratio of PM to ER expression was determined by taking an initial TIRF image of each cell at pH 7.4 followed by acidification of the solution and a subsequent low-pH image. A region of interest encompassing just the cell was

internally thresholded to specifically demarcate the ROI. The ratio of the average intensities (fluorescence at pH 5.5/initial fluorescence at pH 7.4) indicates the fraction of PM fluorescence; smaller values imply higher PM expression.

***Statistical Analysis***

Concentration-response relations for both membrane potential responses from the FlexStation and voltage measurements from electrophysiology were fit to the Hill equation using nonlinear least-squares regression (OriginLab software). Errors for the mean values reported in the text are ± SEM. SEMs for the ratios of two mean values were calculated using a previously published approximation (Motulsky, 2010). Statistical significance was determined by Student's t test. Significant differences are reported at the level of $p<0.05$ (*), $p<0.01$ (**), or $p<0.001$ (***).

# Results

### *β2V287L suppresses LS receptor expression in oocytes*

Previous results for the β2V287L knock-in mouse suggest that the β2V287L mutation selectively reduces the functional expression of LS α4β2* nAChRs in cortical synaptosomes (O'Neill et al., 2013). This reduction could result from an inherent effect of the mutation on the assembly or degradation of LS receptors, or a systemic regulatory response to the mutated receptors that only occurs *in vivo*. To determine whether LS suppression was an inherent property of the β2V287L mutation, we injected oocytes with either α4β2 or α4β2V287L cRNAs in a 1:1 or 10:1 α:β ratio, and measured the ACh concentration-response relations of the expressed receptors. Injecting oocytes with equal amounts of α4 and β2 cRNA yields a mixture of LS and HS α4β2 nAChRs, injecting them with an excess of α4 cRNA favors the formation of LS nAChRs because LS receptors contain three α4 and only two β2 subunits (Zwart and Vijverberg; Moroni et al., 2006), and injecting them with an excess of β2 cRNA favors the formation of HS nAChRs because HS receptors contain more β2 than α4 subunits.

As expected, injecting α4:β2 WT cRNAs in a 1:1 ratio produced a biphasic ACh concentration-response relation (Fig. 3-1C). The data were fit adequately by the sum of two hyperbolic binding functions with $EC_{50}$s differing by >tenfold (Table 1). HS receptors accounted for 65 ± 2% of the maximum WT response (Table 1). In contrast, injecting α4:β2V287L cRNAs in a 1:1 ratio produced a monophasic ACh concentration-response relation that was adequately fit by a single hyperbolic binding function (Fig. 3-1C), suggesting that the β2V287L mutation suppresses LS receptor expression. The $EC_{50}$ of

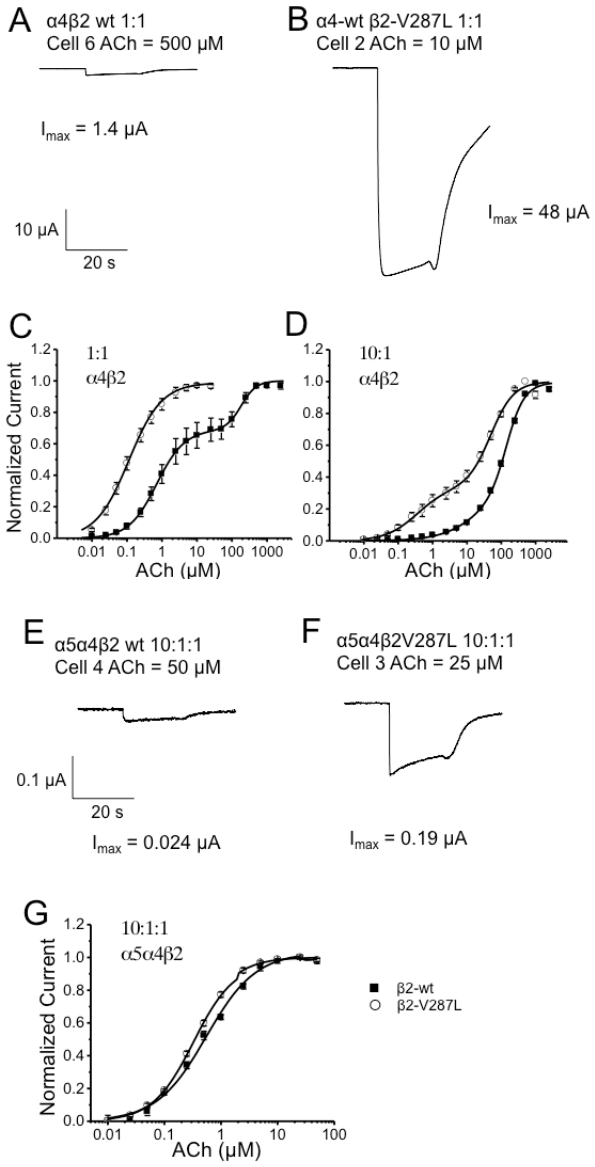


Figure 3-1. Electrophysiological experiments conducted on nAChR constructs expressed in *Xenopus laevis* oocytes. A-B. Representative traces at ACh concentrations eliciting maximal response. C-D. Dose response relations for a (C) 1:1 and (D) 10:1 injection ratio of α4:β2 for both β2-wt and β2-V287L. The β2-V287L mutation biases assembly towards a higher sensitivity receptor, but is still able to form two distinct receptor populations in oocytes. E-F. Sample traces for α5α4β2 injected at a 10:1:1 ratio at ACh doses eliciting maximal response for (E) β2-wt and (F) β2-V287L. G. Dose-response relations for α5α4β2 are not altered by the β2-V287L mutation, providing evidence that the mutation does not alter the ACh sensitivity of α5α4β2 receptors. Solid squares represent β2-wt, and open circles represent β2-V287L conditions.

the α4β2V287L mutant receptor was also significantly ($P < 0.001$) less than that for WT HS receptors (by a factor of sixfold, Table 1). Thus, the β2V287L mutation both increases the ACh sensitivity of HS receptors and suppresses the expression of LS receptors.

Also consistent with previous data (Zwart and Vijverberg; Moroni et al., 2006), injecting α4:β2 cRNAs in a 10:1 ratio shifted the WT ACh concentration-response relation rightward (Fig. 3-1D). To estimate the percentage of HS receptors in this population, we fit the concentration-response relation to the sum of two hyperbolic binding functions by constraining the $EC_{50}$s for the two components to the values obtained from fitting the α4β2 1:1 data (Table 1). Under these constraints, the percent of HS receptors in the population was 7 ± 4% and the percent of LS receptors was 93 ± 4 % (Table 1). Thus, the WT 10:1 ACh concentration-response relation was nearly monophasic. In contrast to the WT, injecting α4:β2V287L cRNAs in a 10:1 ratio produced a pronounced biphasic ACh concentration-response relation (Fig. 3-1D). We fit these data to the sum of two hyperbolic binding functions but constrained the $EC_{50}$ for the HS component to the value obtained by fitting the α4:β2V287L 1:1 data to a single hyperbolic binding component (Table 1). Using this constraint, the mutant HS receptors accounted for 23 ± 3% of the maximum response, and the LS receptors for 77 ± 3% (Table 1). The percentage of mutant HS receptors for the 10:1 injection ratio was significantly larger than the corresponding value for the WT (Table 1). Similar to the effects of the β2V287L mutation on HS receptors, the β2V287L mutation significantly ($P < 0.05$) reduced the $EC_{50}$ for the LS receptors by a factor of fivefold (Table 1). Thus, the β2V287L mutation both inhibits functional LS expression in oocytes even when we use cRNA injection ratios strongly favoring LS expression and also increases the ACh sensitivities of both HS and LS α4β2 receptors by a similar factor.

| **α4β2, ACh, oocytes** | HS $EC_{50}$ | S.E.M. | HS n | S.E.M. | LS $EC_{50}$ | S.E.M. | LS n | S.E.M. | %HS |
|---|---|---|---|---|---|---|---|---|---|
| β2wt | **0.711** | 0.015 | **1.08** | .017 | **143.2** | 15.0 | **1.93** | 0.295 | **67.4%** |
| β2VL | **0.115** | 0.006 | **0.957** | .042 | | | | | **100.0%** |
| β2wt (10α:1β) | **2.39** | 1.61 | **0.827** | 0.46 | **118.0** | 8.48 | **1.39** | 0.11 | **11.4%** |
| VL (10α:1β) | **0.351** | 0.160 | **0.954** | 0.244 | **49.3** | 7.72 | **1.29** | 0.176 | **33.5%** |

Table 3-1. A comparison of two-component Hill function equation fits to ACh dose-response relations in *Xenopus* oocytes injected with α4, and either β2-wt or β2-V287L cRNA. While the mutation results in only one HS population of receptor at a 1:1 injection ratio, it is possible to detect a LS population by biasing stoichiometry towards the LS with a 10α:1β ratio. These data suggest that the LS stoichiometry can form with the mutant β2VL subunit, but that it is heavily unfavored. Parameters correspond to ACh concentration-response relations in Figure 3-1C and D. The $EC_{50}$ and Hill coefficient values represent the mean and SEM. The relative fractions of the high sensitivity component are included in the final column.

| **α5α4β2, ACh, Oocytes** | $EC_{50}$ | S.E.M. | n | S.E.M |
|---|---|---|---|---|
| β2-wt (10:1:1) | **0.514** | 0.0379 | **1.026** | 0.0648 |
| β2-VL (10:1:1) | **0.349** | 0.0081 | **1.181** | 0.0278 |

Table 3-2. Single-component Hill function equation fits to α5α4β2 responses to ACh in *Xenopus* oocytes injected with α5, α4, and either β2-wt or β2-VL cRNA. No significant differences were found, indicating that incorporation of the β2-VL subunit does not alter the sensitivity or Hill coefficient of the α5α4β2 receptor.

Previous results show that the α5 nicotinic subunit co-assembles with α4 and β2 to form a highly ACh-sensitive nicotinic receptor (Brown et al., 2007; (Kuryatov et al., 2008). To determine whether the β2V287L mutation increased the ACh sensitivity of α5α4β2 nAChRs, we injected oocytes with α5, α4, and either β2-WT or β2-V287L cRNAs with a large excess of α5 (α5:α4:β2 ratio of 10:1:1) and measured the ACh concentration-response relations of the expressed receptors (Fig. 3-1E, F, and G). The WT and mutant ACh concentration-response relations of the expressed receptors were monophasic (Fig. 3-1G), and fit adequately by single hyperbolic binding components with $EC_{50}$s similar to those obtained for the mutant and WT α4β2 HS receptors (Table 3-1). The β2V287L mutation did not significantly affect the $EC_{50}$ of α5α4β2 nAChRs (Table 3-2) even though it significantly reduced the $EC_{50}$ of α4β2 nAChRs, suggesting that the mutation does not increase the ACh sensitivity of α5* nAChRs.

***β2V287L reduces the maximum α4β2 response in HEK cells***

The β2V287L mutation reduces the maximum agonist response of synaptosomal α4β2* nAChRs in mice (O'Neill et al., 2013). To determine whether it had a similar effect on expressed α4β2 nAChRs, we transfected HEK cells with α4β2 (WT) or α4β2V287L (mutant) cDNAs and measured the responses of the expressed receptors to 5 and 300 μM ACh using a fluorescent membrane potential assay (Fig. 3-2). For the WT receptors, the peak amplitude of the 5 μM response was roughly half that of the 300 μM response (Fig. 3-2a). In contrast, the peak amplitude of the mutant 5 μM response was not significantly different from that of the 300 μM response, suggesting that 5 μM is nearly a saturating concentration of ACh for the mutant receptors (Fig. 3-2a). The response of the mutant

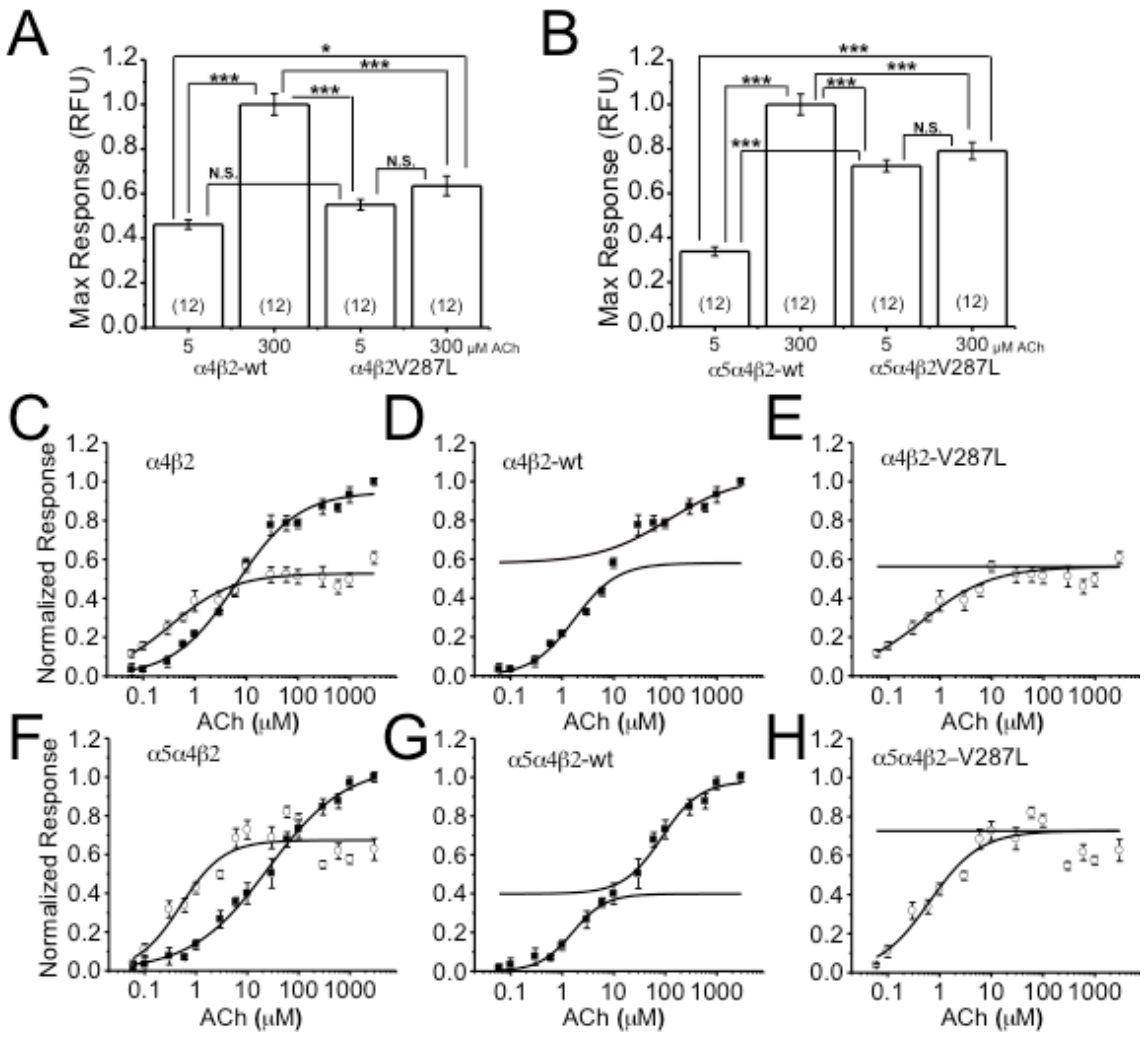


Figure 3-2. Maximal responses at given concentrations and dose-repsonse relations were obtained using a FlexStation III membrane potential dye kit. Solid squares represent β2-wt, and open circles represent β2-V287L conditions. Statistics were performed with one-way ANOVA with post-hos Tukey test. * = $p<0.05$; **=$p<0.01$; ***=$p<0.001$.

| **ACh, HEK cells** | HS $EC_{50}$ | S.E.M. | HS n | S.E.M. | LS $EC_{50}$ | S.E.M. | LS n | S.E.M. | %HS |
|---|---|---|---|---|---|---|---|---|---|
| α4β2-WT | **1.72** | 0.24 | **1.05** | 0.13 | **91.27** | 28.2 | **0.69** | 0.16 | **58.0%** |
| α4β2V287L | **0.45** | 0.081 | **0.65** | 0.09 | | | | | **100.0%** |
| α5α4β2-WT | **1.58** | 0.17 | **1.35** | 0.161 | **85.12** | 19.8 | **1.16** | 0.282 | **39.9%** |
| α5α4β2V287L | **0.636** | 0.106 | **0.888** | 0.129 | | | | | **100.0%** |

Table 3-3. A comparison of two-component Hill function equation fits to ACh dose-response relations in HEK cells obtained using a FlexStation III and membrane potential dye kit. Cells were transfected with α4, and either β2-WT or β2V287L DNA at a 1:1 ratio, or α5, α4, and either β2 variant in a 1:1:1 ratio. The β2V287L mutation results in loss of the LS component in mammalian cells when α5 is present or not. Parameters correspond to ACh concentration-response relations in Figure 3-2. The $EC_{50}$ and Hill coefficient values represent the mean and standard error. The relative fractions of the high sensitivity component are included in the final column.

receptors to 300 μM ACh was also ~40% smaller than the WT. Thus, β2V287L reduced the maximum ACh response of α4β2 nAChRs expressed in HEK cells by >50% and increased the overall sensitivity of the ACh response. These results are consistent with the mutant-induced reduction in the proportion of functionally expressed LS α4β2 nAChRs measured above in oocytes and show that a mutant-induced reduction in the maximum ACh response occurs in a mammalian expression system.

We also measured full ACh concentration-response relations for HEK cells transiently transfected with α4β2 (1:1 ratio), α4β2V287L (1:1), α5α4β2(1:1:1), and α5α4β2V287L (1:1:1) cDNAs (Fig. 3-2). The data were fit to two-component Hill function equations (Table 3-3 and 3-4). The β2V287L mutation significantly reduced the $EC_{50}$ and maximum response of the ACh concentration response relation relative to the WT control (Table 3-3). Co-expression with α5 did not significantly affect the WT or mutant $EC_{50}$s (Table 3-4). The Hill coefficients of the four concentration-response relations were also not significantly different. Thus, consistent with the oocyte experiments, β2V287L

increased overall ACh sensitivity and reduced the maximum response of α4β2 nAChRs expessed in HEK cells.

***α5 co-expression produces an increase in the mutant response relative to the WT***

Previous results show that co-expression of the ADNFLE mutant α4S247F subunit with the WT β2 subunit in HEK cells does not produce functional nicotinic receptors unless an accessory nicotinic subunit such as α5 is added (Kuryatov et al., 2008). Our results show that HEK cells express functional α4β2V287L receptors without the need for an additional accessory subunit but the maximum ACh response of these receptors is less than that of the WT (Fig. 3-2A). To determine whether α5 co-expression improves functional α4β2V287L expression relative to the WT, we transfected HEK cells with α5α4β2 or α5α4β2V287L cDNA and measured the responses of the expressed receptors to 5 and 300 μM ACh using a fluorescent membrane potential assay. Similar to the α4β2 WT response, the peak responses of cells transfected with WT α5, α4, and β2 subunits (1:1:1 ratio) to 5 μM ACh was > 50% smaller than the 300 mM ACh response (Fig. 3-2B). In contrast, the response of cells transfected with α5, α4, and β2V287L subunits (1:1:1) to 5 μM and 300 μM ACh were not significantly different, again suggesting that 300 μM ACh is close to saturation for the mutant receptors. Consistent with previous results for α4S247F ADNFLE mutation, α5 co-expression appeared to increase the mutant 300 μM ACh response relative to the WT. To test whether this increase was significant, we compared the ratio of the mutant to WT 300 μM ACh response with, and without, α5 co-expression (Fig. 3-3). The ratio of the α5α4β2V287L to α5α4β2-WT at 300 μM ACh response (0.79 ± 0.05, n= 24 wells) was significantly larger ($p < 0.05$) than that of the α4β2V287L to α4β2 response

(0.64 ± 0.05, n= 24 wells). Thus, consistent with the previously reported effect of a α5 co-expression on β2* nAChRs containing the α4S247F ADNFLE mutation, α5 significantly increased the functional expression of α4β2V287L* nAChRs relative to the WT control.

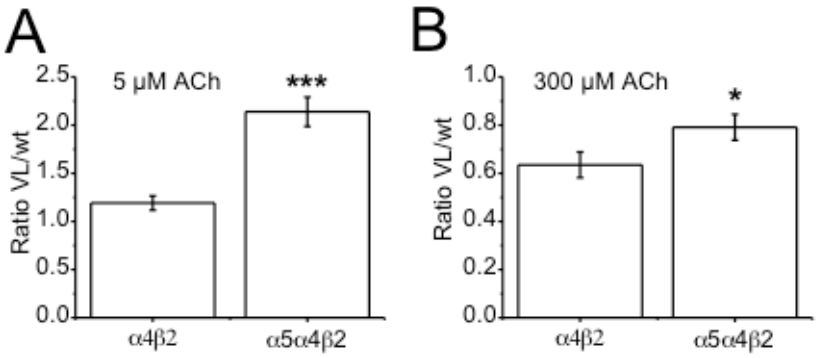


Figure 3-3. FlexStation membrane potential assay comparing the magnitude of response to ACh of receptors containing mutant β2V287L to β2-WT. The β2V287L mutation increases the change in membrane potential upon agonist addition to a greater degree in cells transfected with α5α4β2 than α4β2 at both 5 and 300 μM ACh, doses that activate the HS, and HS+LS, respectively. These data suggest that the β2V287L subunit increases the incorporation of α5 subunits into PM receptors.

***β2V287L reduces the $EC_{50}$ and maximum response of α4β2 nAChRs in N2a cells***

To validate the results of the fluorescent membrane potential measurements, we measured the effects of the b2V287L mutation on the ACh concentration-response relations of α4β2 and α4β2V287L nAChRs expressed in a different mammalian cell line (N2a cells), using whole-cell patch clamping. ACh was applied to the cells using a rapid microperfusion system to minimize agonist-induced desensitization. The voltage-clamp concentration-response data were fit to three-parameter Hill equations (Fig. 3-4,E-F and Table 3-4). The β2V287L mutation shifted the overall ACh concentration-response relation to the left. The α4β2V287L $EC_{50}$ was 0.4 ± 0.1 μM compared to 30 ± 20 μM for the α4β2-WT value. The

Hill coefficients for both the mutant (0.7 ± 0.2) and WT receptors (0.6 ± 0.1) were less than unity, suggesting receptor heterogeneity in both cases. Due to the limited number of ACh concentrations tested (8 and 9 for WT and mutant, respectively), a two-component fit may be a less meaningful analysis of these data in compared to those from HEK and oocytes experiments. The peak α4β2V287L response to 1 μM ACh (650 ± 230 pA, n = 9 cells) was significantly greater ($P < 0.05$) than the α4β2 WT value (100 ± 20 pA, n = 8) (Fig. 3-5B) but the α4β2V287L maximum response (900 ± 240 pA, n = 9) was significantly ($P < 0.05$) less than the WT value (1800 ± 400 pA, n = 8) (Fig. 3-4H). In summary, β2V287L reduced the overall $EC_{50}$ of the ACh concentration-response relation and the maximum response, and increased the amplitude of peak ACh response at concentrations near the foot of the WT concentration-response relation (1 μM). Thus, the mutation does not uniformly reduce the ACh response throughout the entire concentration-response relation.

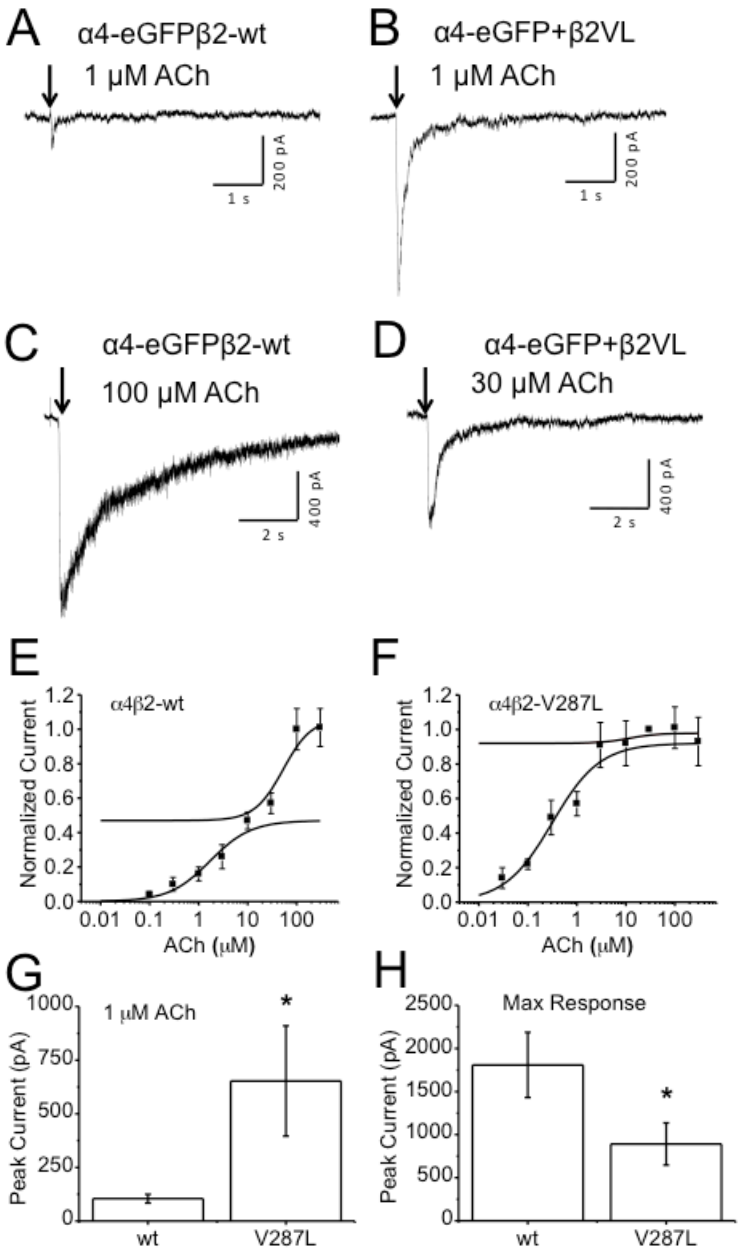


Figure 3-4. Electrophysiology was performed in N2a cells transiently transfected with α4-eGFP and either β2-WT or β2V287L cDNA. A-D. Sample traces at varying doses. E-F. Dose-response relations show that β2V287L shifts the EC50 to the left. These data are consistent with a loss of the LS receptor population, but are limited by the low number of doses tested (8 for WT and 9 for the mutant). G. At 1 μM ACh, peak currents are significantly higher with mutant. H. However, at doses of ACh eliciting a maximal response, the mutant peak current is half that of the WT receptor. These data are consistent with the mutant causing increased sensitivity, selective loss of the LS population, and about half of the total amount of receptors on the PM.

| **α4β2, ACh, N2a** | HS $EC_{50}$ | S.E.M. | HS n | S.E.M. | LS $EC_{50}$ | S.E.M. | LS n | S.E.M. | %HS |
|---|---|---|---|---|---|---|---|---|---|
| α4β2-WT | **1.70** | 0.41 | **1.04** | 0.249 | **52.65** | 13.2 | **1.5** | 3.88 | **47.0%** |
| α4β2V287L | **0.31** | 0.070 | **0.89** | 0.167 | **11.8** | 40.8 | **1.5** | 9.9 | **91.1%** |

Table 3-4. A comparison of two-component Hill function equation fits to ACh dose-response relations in N2a cells transiently transfected with α4-eGFP and either β2-WT or β2V287L cDNA. These fits were performed on data displayed in Figure 3-4. The parameters shown here are consistent with the β2V287L mutation causing a leftward shift in $EC_{50}$, selective loss of the LS component, and resulting reduction of total PM receptors by half. However, these data should be interpreted with caution due to the low number of ACh concentrations over which the function is fitted.

### *β2V287L reduces surface receptor expression and alters subunit stoichiometry*

The decrease in the maximum response and suppression of the LS component of ACh concentration-response relation suggest that β2V287L reduces the total number of α4β2 nAChRs expressed on the PM and alters their subunit stoichometry. However, mutant-induced changes in the single-channel conductance, agonist desensitization, and agonist efficacy of HS and LS mutant receptors could contribute to these two effects. We used SEP-tagged subunits to independently determine whether the β2V287L mutation affected the number and subunit stoichiometry of α4β2 receptors expressed on the PM.

To ensure that α4 and β2 subunits expressed in the PM were incorporated into receptors, we asked whether individual α4 and β2 SEP-tagged subunits could be expressed on the cell surface without co-transfection of the complementary subunit (Fig. 3-5). We found that individual subunits, without the complementary subunit required to form a pentamer, did not reach the PM. Transfection with either WT α4-SEP or β2-SEP alone resulted in easily detectable fluorescent protein inside the cell but almost none on the

plasma membrane (Fig. 3-5B). Thus, in the absence of the complementary subunit, almost all α4 and β2 protein remains inside the cell in the ER.

We then measured the effects of the β2V287L mutation on surface α4-SEP and β2-SEP expression in cells transfected with both subunits (Fig. 3-6). The β2V287L mutation significantly reduced the surface expression of both subunits. Surface fluorescence for the α4-SEP subunit of the mutant receptors was 36 ± 6 % (n = 54 cells) that of the WT receptors. Surface fluorescence of the β2V287L-SEP subunit was 60 ± 8 % (n = 54) that of the WT β2 subunit. Thus, the mutation reduced the surface expression of both subunits but the fractional reduction in PM α4 subunits was more than that for β2. If the mutation simply reduced the number of surface receptors without altering their subunit stoichiometry, then the number of α4-SEP and β2V287L-SEP subunits in the mutant receptors would decline by the same percentage. However, there was a significantly greater ($P < 0.05$) decrease in the percentage of α4-SEP on the cell surface than β2-SEP. Thus, the β2V287L mutation reduced both the total number of surface receptors and the mean number of α4 subunits incorporated into individual mutant surface receptors.

We can estimate the mutant-induced reduction in total surface receptors and the proportion of HS receptors in the WT surface receptor population from the mutant-induced reductions in α4-SEP and β2-SEP surface expression by making two simplifying assumptions (depicted in Fig. 3-7). First, we assume that the α4β2 subunit ratio for the WT HS receptors is 2:3, and that for the LS receptors is 3:2. This assumption is consistent with previous studies (Zwart and Vijverberg, 1998; Moroni et al., 2006). Second, we assume that mammalian cell lines transfected with equal amounts of α4 and β2V287L cDNA (w/w) express express only HS receptors in the plasma membrane, and their α:β subunit

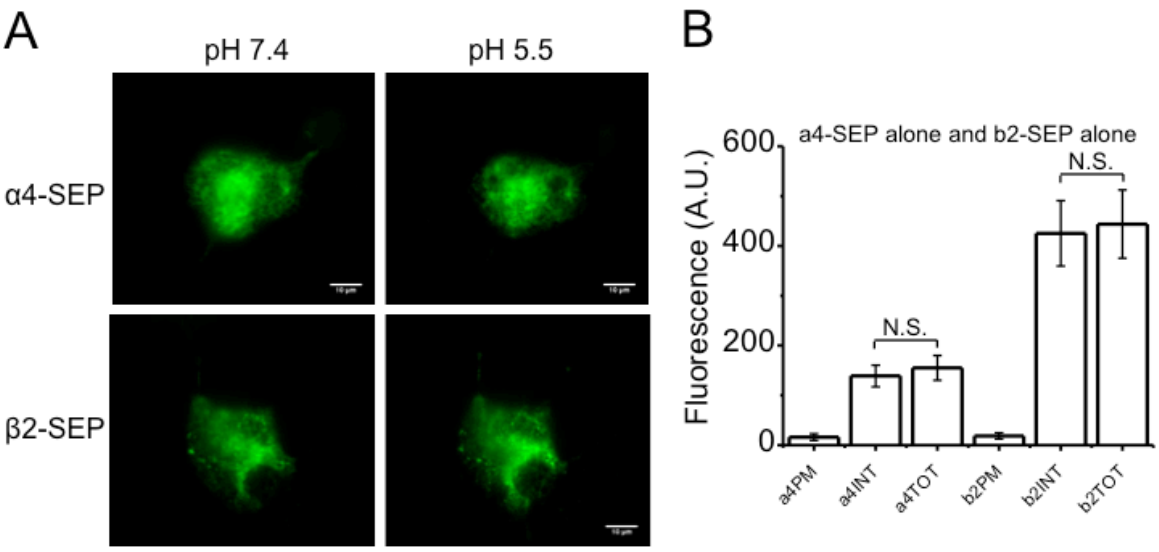


Figure 3-5. Single SEP-tagged nAChR subunits do not reach the plasma membrane. A. Representative images of either α4-SEP and β2-SEP transiently transfected into N2a cells without the complementary subunit. B. Minimal quenching occurs upon perfusion with acidic extracellular solution, indicating a lack of SEP-containing single subunits on the PM. This control experiment demonstrates the ability of the SEP assay to detect PM populations of SEP tagged nAChR subunits.

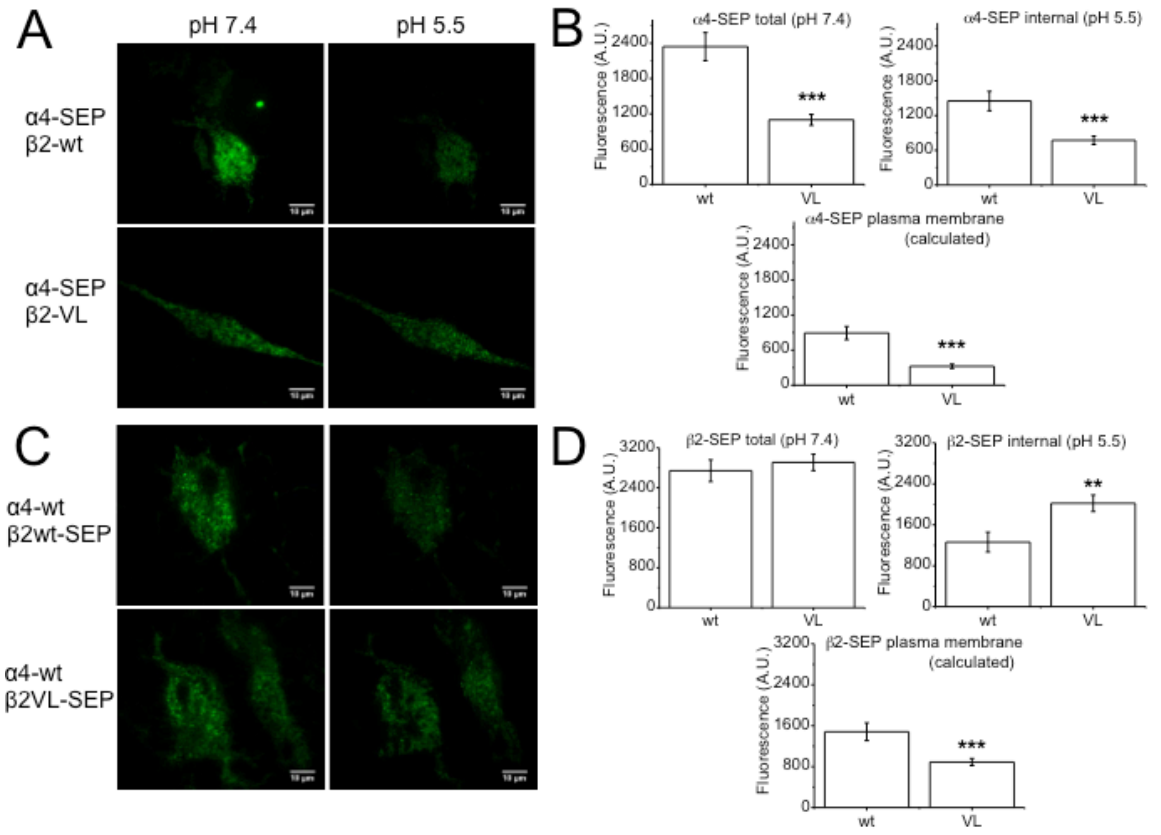


Figure 3-6. The β2V287L mutation causes a ~60% decrease in PM levels of α4, and a ~60% decrease in β2. A and C. Representative images of N2a cells transiently transfected with an SEP-tagged subunit and the complementary subunit. B. The β2V287L mutation results in a decline in the amount of total α4-SEP, which is seen both on the plasma membrane and interior to the cell. D. The mutation results in a smaller decrease in the β2 population on the PM, and an increase in the amount of β2 inside the cell. These data are consistent with the hypothesis that the mutation inhibits the incorporation of the α4 subunit into the accessory position, possibly leading to an increased rate of degradation, which could account for the overall lower total level of a α4-SEP when co-transfected with the β2V287L mutant subunit.

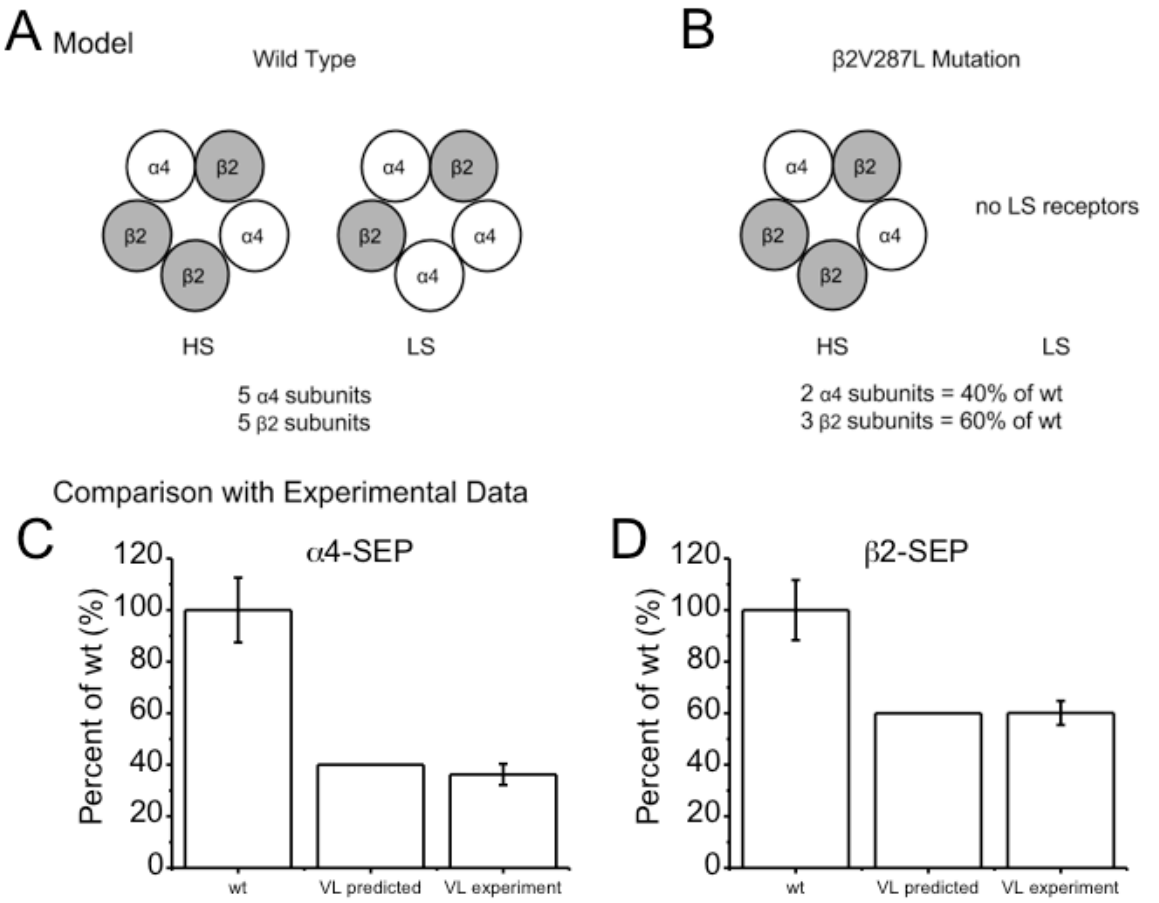


Figure 3-7. Our model shows excellent agreement between predicted and experimental data, demonstrating that the β2V287L mutation results in loss of the lower sensitivity (LS) population of receptors on the PM, but does not affect levels of the higher sensitivity (HS) receptor on the PM. Upon loss of all LS receptors, and no change in HS number, a 60% decrease in α4-SEP, and a 40% decrease in β2-SEP is expected, which agrees with experimental data.

ratio is 2:3 (identical to WT HS receptors). Using these two assumptions, the number of surface WT α4 subunits ($a_{WT}$) is:

$$\alpha_{WT}=T_{WT}[2(x)+3(1-x)],$$

where $T_{WT}$ is the total number of α4β2 surface receptors, $x$ is the fraction of HS receptors, 2($x$) is the number of a subunits in surface HS receptors, and 3(1-$x$) is the number in surface LS receptors. The number of mutant surface α4 subunits ($\alpha_M$) is simply:

$$\alpha_M=2T_M,$$

where $T_M$ is the total number of mutant α4β2V287L surface receptors. Taking the ratio of these two values ($\alpha_M/\alpha_{WT}$) and simplifying, we have:

$$\frac{\alpha_M}{\alpha_{WT}}=\frac{2T_M}{T_{WT}(3-x)}. \qquad \text{Eq. 1}$$

The number of surface WT β2 subunits ($\beta_{WT}$) is:

$$\beta_{WT}=T_{WT}[3(x)+2(1-x)].$$

The number of mutant surface β2V287L subunits ($\beta_M$) is:

$$\beta_M=3T_M.$$

Taking the ratio of $\beta_M$ to $\beta_{WT}$ and simplifying, we have:

$$\frac{\beta_M}{\beta_{WT}}=\frac{3T_M}{T_{WT}(2+x)}. \qquad \text{Eq. 2}$$

Dividing $\alpha_M/\alpha_{WT}$ by $\beta_M\beta b_{WT}$ , we have:

$$\frac{\frac{\alpha_M}{\alpha_{WT}}}{\frac{\beta_M}{\beta_{WT}}}=\frac{2(x+2)}{3(x-3)} \qquad \text{Eq.3}$$

Solving Eq. 3 for $x$ yields:

$$x=\frac{3\frac{\alpha_M\beta_{WT}}{\alpha_{WT}\beta_M}-\frac{4}{3}}{\frac{\alpha_M\beta_{WT}}{\alpha_{WT}\beta_M}+\frac{2}{3}} \qquad \text{Eq. 4}$$

Substituting the mean values for $\alpha_M/\alpha_{WT}$ (0.36) and $\beta_M/\beta_{WT}$ (0.6) obtained above in Eq. 4 gives a value of 0.37 for $x$. Solving Eq. 2 for $T_M/T_{WT}$, we have:

$$\frac{(x+2)}{3}\frac{\beta_M}{\beta_{WT}} = \frac{T_M}{T_{WT}}. \qquad \text{Eq. 5}$$

Substituting a value of 0.37 for $x$ and 0.60 for $\beta_M/\beta_{WT}$ in Eq. 2 gives a value of 0.47 for $T_M/T_{WT}$. According to this analysis, the β2V287L mutation reduced the total number of α4β2 nAChRs expressed on the plasma membrane of HEK cells by 53% ((1-0.47) X 100) and HS receptors account for 37% of the WT α4β2 nAChRs expressed in the plasma membrane of HEK cells. Thus, the β2V287L mutation reduces surface receptor expression and alters the subunit stoichiometry of these receptors.

***The β2V287L Mutation increases α5 surface expression***

The fluorescent membrane potential data suggest that α5 increases the number of α4β2V287L* mutant nAChRs expressed on the cell surface (Fig. 3-2B & 3-3). To test this hypothesis, we co-expressed α5-SEP with α4 and either β2-WT or β2V287L in N2a cells and measured the total, internal, and PM α5-SEP fluorescence (Fig. 3-8). Co-expression with α4 and β2V287L subunits increased α5-SEP PM fluorescence nearly fourfold compared to co-expression with the α4 and β2-WT subunits. However, it did not significantly affect internal α5-SEP fluorescence. The increase in total fluorescence was due largely to the effect of the mutation on PM fluorescence. Thus, β2V287L enhances the incorporation of α5 into α4β2* surface nAChRs. This effect may explain the relative increase in the maximal ACh response of mutant α5α4β2V287L receptors compared to the WT α5α4β2 receptors (Fig 3-3 and Fig. 3-2B).

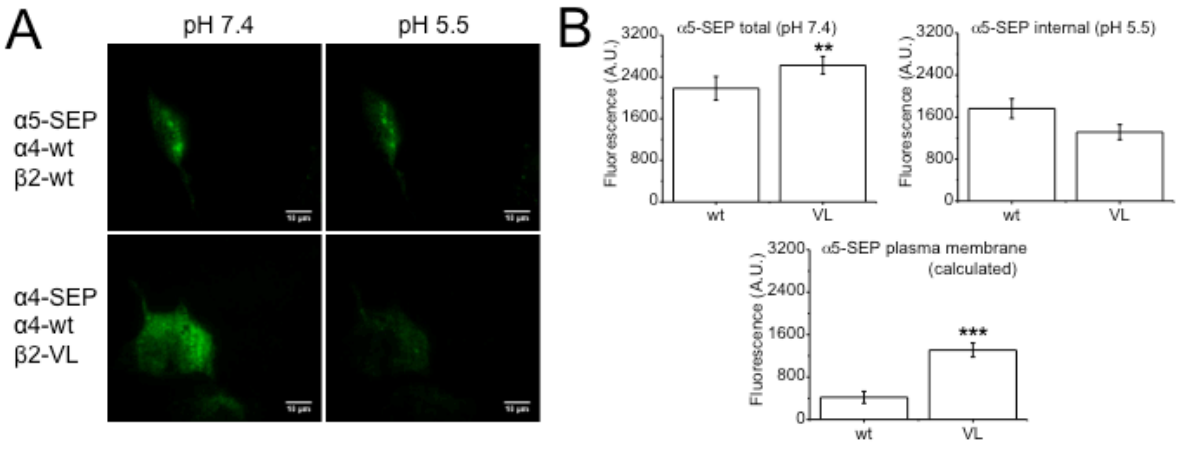


Figure 3-8. The β2V287L mutation increases plasma membrane expression of α5. A. Representative images of N2a cells transfected with α5-SEP, α4, and either β2-WT or β2V287L cDNA at pH 7.4 and 5.5. B. The β2V287L mutation caused an increase in both the total and PM fluorescence of α5-SEP, but not a significant change in the level of α5-SEP inside the cell.

# Discussion

Our main findings are that the β2V287L ADNFLE mutation reduces the proportion of LS α4β2 nAChRs expressed in the PM but increases the ACh sensitivities of both the HS and LS α4β2 nAChRs. These changes produce a leftward shift in the overall α4β2 ACh concentration-response relation and a reduction in the maximum response. Despite reducing the maximum response, the β2V287L mutation actually increases the size of the voltage-clamped ACh response to a sub-saturating ACh concentration (1 μM). Previous experiments on mice with partial genetic deletions of the α4 or β2 nicotinic subunits show that HS and LS α4β2 nAChRs are expressed *in vivo* (Gotti et al., 2008). In mice, β2V287L increases the ACh sensitivities of both HS and LS α4β2* nAChRs in brain synaptosomes and suppresses the functional expression of α4β2* LS receptors (O'Neill et al., 2013). Our data show that the effects of the β2V287L mutation on α4β2* nAChRs *in situ* can be replicated with heterologously expressed receptors. Thus, they appear to be caused by a direct effect of the mutation on the assembly and function of α4β2 nAChRs rather than by system-level changes in the regulation of α4β2 receptor expression.

The use of SEP-tagged subunits is a novel approach that allows us to study the effects of ADNFLE mutations on the PM expression and subunit stoichiometry of nicotinic receptors without relying on functional data. Results from the SEP experiments independently confirm three important conclusions of the electrophysiological and fluorescent membrane potential experiments. First, β2V287L reduces the total number of α4β2 nAChRs expressed in the PM. A previous PET study of ADNFLE patients with the α4S284F and β2V287L mutations shows that these mutations also reduce nAChR density

in the right dorsolateral prefrontal cortex (Picard et al., 2006). Second, β2V287L reduces the mean number of β2 subunits per receptor (which is consistent with a reduction in the proportion of LS receptors in the population). Finally, SEP data show that β2V287L increases the number of α5 subunits in the PM of cells transfected with α5, α4, and β2 subunits, suggesting that the mutation increases α5α4β2 nAChR surface expression.

The sole previous study of how ADNFLE mutations affect the subunit stoichiometry of α4β2 nAChRs suggests that they increase the proportion of $(\alpha4)_3(\beta2)_2$ (LS) receptors in the population (Son et al., 2009). This conclusion is based on Forster resonance energy transfer (FRET) measurements between combinations of GFP and mCherry tagged α4 and β2 subunits. A possible reason for the apparent discrepancy between these previous data and our SEP data is that the previous FRET experiments measure apparent changes in stoichiometry for all subunits, including those expressed inside the cell rather than exclusively on in the PM. Our SEP data provide a more direct measurement of changes in amounts of subunit proteins expressed on the cell surface than the FRET measurements conducted previously. Moreover, the SEP data are consistent with the functional data from *Xenopus* oocytes and two types of mammalian cell lines, HEK and N2a. These data, taken together, provide strongly support the conclusion that the β2V287L mutation suppresses the surface expression of LS α4β2 nAChRs.

Similar to the α4S247F ADNFLE mutation (Kuryatov et al., 2008), co-expression of WT α4 and mutant β2V287L subunits with the α5 subunit improves surface expression of the mutant receptor relative to the α5α4β2-WT. An α4 subunit is thought to occupy the accessory subunit position in the LS α4β2 pentamer. In contrast, β2 and α5 subunits occupy comparable positions in the HS α4β2 nAChR and α5α4β2 nAChR, respectively. Thus,

β2V287L-mediated suppression of LS expression suggests that the mutation inhibits the inclusion of α4 subunits in the accessory position. The predicted *in vivo* effects of the mutation are a loss of LS α4β2 nAChRs in the mutant mouse, but a sparing (or even an increase) of α5α4β2. In contrast to its effect on α4β2 nAChRs, the mutation does not appear to affect the ACh sensitivity of α5α4β2 receptors.

Two previously reported effects of the ADNFLE mutations may result from LS suppression—reduced $Ca^{2+}$ potentiation of the α4β2 ACh response and an increase in the Hill coefficient for the α4β2 ACh concentration-response relation. If $Ca^{2+}$ potentiates the response of HS receptors less than it does LS receptors, then suppressing LS expression would be expected to reduce $Ca^{2+}$ potentiation of the overall α4β2 ACh response, particularly in the upper range of the concentration-response relation where the HS response dominates. Thus, reduced $Ca^{2+}$ potentiation may be a consequence of reduced LS α4β2 expression. The previously reported increase in the Hill coefficients of the α4S248Fβ2 and α4(777ins3)β2 ACh concentration-response relations relative to WT control may also be a consequence of LS suppression (Figl et al., 1998). We would expect LS suppression to increase the homogeneity of the receptor population and, thus, increase the Hill coefficient of the overall ACh concentration-response relation.

Despite strong genetic evidence linking α4 and β2 nicotinic subunit mutations to ADNFLE, the pathophysiology of the disease is still poorly understood. Previous experiments using conditionally-expressed transgenic β2V287L mouse models suggest that alterations in brain development, rather than acute activation of the mutant receptors, evoke seizure activity (Manfredi et al., 2009). Silencing the β2V287L mutant transgene during early development prevents the occurrence of seizures in adult mice despite expression of

the mutant transgene in the adult (Manfredi et al., 2009). Thus, inactivating the conditionally expressed mutant transgene during early development suffices to prevent the onset of seizures in the adult. In contrast, silencing the transgene in adult mice does not prevent seizure activity. Previous studies of brain development show that β2* nAChRs regulate the development of excitatory synaptic transmission in the cortex (Ballesteros-Yáñez et al., 2010; (Lozada et al., 2012). Genetic deletion of the β2 subunit reduces dendritic spine density in pyramidal neurons in the prelimbic/infralimbic area (Ballesteros-Yáñez et al., 2010) and causes a redistribution of glutamatergic synapses from dendritic spines to the dendritic shaft in pyramidal neurons. In contrast, the activation of β2* nAChRs by nicotine during early development increases spine formation in the dendrites of pyramidal neurons (Lozada et al., 2012). Our results show that β2V287L increases the response of α4β2 nAChRs expressed in HEK cells to sub-saturating ACh (1 μM), even though the mutation reduces the overall maximum ACh response. Thus, an increased mutant β2* nAChR response to sub-saturating ACh may enhance seizure susceptibility by altering the normal course of development for excitatory synaptic transmission in the brain.

The suppression of LS α4β2 nAChR expression may contribute to ADNFLE epileptogenesis. The presence of both HS and LS α4β2 nAChRs in the same presynaptic nerve terminal would be expected to enhance the dynamic range of the presynaptic nicotinic response (Harpsøe et al., 2011). Presynaptic nAChRs on cholinergic nerve terminals in the cortex act as autoreceptors that facilitate ACh release (Ochoa and O'Shea, 1994; (Quirion et al., 1994). In the absence of LS receptors, the response of these receptors may quickly saturate as the firing frequency of presynaptic cholinergic neurons escalates. Consequently, the loss of presynaptic LS nAChRs may limit the ability of ACh release

from cholinergic neurons to follow high-frequency stimulation. ACh release in the cortex can inhibit firing in postsynaptic neurons by activating muscarinic receptors. Reducing the firing frequency at which this inhibitory muscarinic response saturates could be proepileptic because it impairs muscarinic-mediated inhibitory feedback in the brain and/or the development of inhibitory feedback networks.

In conclusion, our results show that the β2V287L ADNFLE mutation increases the ACh sensitivities of both HS and LS α4β2, but not α5α4β2 nAChRs. It also suppresses LS α4β2 expression. LS suppression may be a common feature of the ADNFLE mutations and could potentially explain their previously reported effects on $Ca^{2+}$ potentiation of the ACh response. Both these effects may contribute to ADNFLE epileptogenesis by altering the development of excitatory synaptic connections in the brain and/or impairing the ability of presynaptic nAChR autoreceptors to properly regulate cortical ACh release.

# References

Ballesteros-Yáñez I, Benavides-Piccione R, Bourgeois J-P, Changeux J-P, and DeFelipe J (2010) Alterations of cortical pyramidal neurons in mice lacking high-affinity nicotinic receptors. Proceedings of the National Academy of Sciences 107:11567-11572.

Brown RW, Collins AC, Lindstrom JM, and Whiteaker P (2007) Nicotinic α5 subunit deletion locally reduces high-affinity agonist activation without altering nicotinic receptor numbers. J Neurochem 103:204-15.

De Fusco M, Becchetti A, Patrignani A, Annesi G, Gambardella A, Quattrone A, Ballabio A, Wanke E, and Casari G (2000) The nicotinic receptor b2 subunit is mutant in nocturnal frontal lobe epilepsy. Nat Genet 26:275-6.

Ferini-Strambi L, Sansoni V, and Combi R (2012) Nocturnal frontal lobe epilepsy and the acetylcholine receptor. The neurologist 18:343-349.

Figl A, Viseshakul N, Shafaee N, Forsayeth J, and Cohen BN (1998) Two mutations linked to nocturnal frontal lobe epilepsy cause use-dependent potentiation of the nicotinic ACh response. J Physiol (Lond) 513:655-70.

Gotti C, Moretti M, Meinerz N, Clementi F, Gaimarri A, Collins AC, and Marks MJ (2008) Partial deletion of the nicotinic cholinergic receptor α4 and β2 subunit genes changes the acetylcholine sensitivity of receptor mediated $^{86}Rb^{+}$ efflux in cortex and thalamus and alters relative expression of α4 and β2 subunits. Mol Pharmacol.

Harpsøe K, Ahring PK, Christensen JK, Jensen ML, Peters D, and Balle T (2011) Unraveling the high-and low-sensitivity agonist responses of nicotinic acetylcholine receptors. The Journal of Neuroscience 31:10759-10766.

Heron SE, Smith KR, Bahlo M, Nobili L, Kahana E, Licchetta L, Oliver KL, Mazarib A, Afawi Z, and Korczyn A (2012) Missense mutations in the sodium-gated potassium channel gene KCNT1 cause severe autosomal dominant nocturnal frontal lobe epilepsy. Nature genetics 44:1188-1190.

Kurth S, Ringli M, Geiger A, LeBourgeois M, Jenni OG, and Huber R (2010) Mapping of cortical activity in the first two decades of life: a high-density sleep electroencephalogram study. The Journal of Neuroscience 30:13211-13219.

Kuryatov A, Onksen J, and Lindstrom J (2008) Roles of accessory subunits in α4β2α5 nicotinic receptors. Mol Pharmacol 74:132-43.

Lozada AF, Wang X, Gounko NV, Massey KA, Duan J, Liu Z, and Berg DK (2012) Glutamatergic synapse formation is promoted by α7-containing nicotinic acetylcholine receptors. The Journal of Neuroscience 32:7651-7661.

Manfredi I, Zani AD, Rampoldi L, Pegorini S, Bernascone I, Moretti M, Gotti C, Croci L, Consalez GG, and Ferini-Strambi L (2009) Expression of mutant β2 nicotinic receptors during development is crucial for epileptogenesis. Human molecular genetics 18:1075-1088.

Miesenbock G, De Angelis DA, and Rothman JE (1998) Visualizing secretion and synaptic transmission with pH-sensitive green fluorescent proteins. Nature 394:192-5.

Moroni M, Zwart R, Sher E, Cassels BK, and Bermudez I (2006) α4β2 nicotinic receptors with high and low acetylcholine sensitivity: pharmacology, stoichiometry, and sensitivity to long-term exposure to nicotine. Mol Pharmacol 70:755-68.

Motulsky H. (2010). Intuitive biostatistics: a nonmathematical guide to statistical thinking: Oxford University Press).

O'Neill HC, Laverty DC, Patzlaff NE, Cohen BN, Fonck C, McKinney S, McIntosh JM, Lindstrom JM, Lester HA, Grady SR, and Marks MJ (2013) Mice expressing the ADNFLE valine 287 leucine mutation of the β2 nicotinic acetylcholine receptor subunit display increased sensitivity to acute nicotine administration and altered presynaptic nicotinic receptor function. Pharmacology, biochemistry, and behavior 103:603-21.

Ochoa EL, and O'Shea SM (1994) Concomitant protein phosphorylation and endogenous acetylcholine release induced by nicotine: dependency on neuronal nicotinic receptors and desensitization. Cellular and molecular neurobiology 14:315-340.

Picard F, Bruel D, Servent D, Saba W, Fruchart-Gaillard C, Schöllhorn-Peyronneau M-A, Roumenov D, Brodtkorb E, Zuberi S, and Gambardella A (2006) Alteration of the in vivo nicotinic receptor density in ADNFLE patients: a PET study. Brain 129:2047-2060.

Quirion R, Richard J, and Wilson A (1994) Muscarinic and nicotinic modulation of cortical acetylcholine release monitored by in vivo microdialysis in freely moving adult rats. Synapse 17:92-100.

Richards CI, Srinivasan R, Xiao C, Mackey ED, Miwa JM, and Lester HA (2011) Trafficking of α4* nicotinic receptors revealed by superecliptic phluorin: effects of a β4 amyotrophic lateral sclerosis-associated mutation and chronic exposure to nicotine. J Biol Chem 286:31241-9.

Rodrigues-Pinguet N, Jia L, Li M, Figl A, Klaassen A, Truong A, Lester HA, and Cohen BN (2003) Five ADNFLE mutations reduce the $Ca^{2+}$ dependence of the a4b2 acetylcholine response. J Physiol 550:11-26.

Rodrigues-Pinguet NO, Pinguet TJ, Figl A, Lester HA, and Cohen BN (2005) Mutations linked to autosomal dominant nocturnal frontal lobe epilepsy affect allosteric $Ca^{2+}$ activation of the a4b2 nicotinic acetylcholine receptor. Mol Pharmacol 68:487-501.

Sansoni V, Forcella M, Mozzi A, Fusi P, Ambrosini R, Ferini-Strambi L, and Combi R (2013) Functional characterization of a CRH missense mutation identified in an ADNFLE family. PloS one 8:e61306.

Scheffer IE, Bhatia KP, Lopes-Cendes I, Fish DR, Marsden CD, Andermann E, Andermann F, Desbiens R, Keene D, Cendes F, and et al. (1995) Autosomal dominant nocturnal frontal lobe epilepsy. A distinctive clinical disorder. Brain 118:61-73.

Son CD, Moss FJ, Cohen BN, and Lester HA (2009) Nicotine normalizes intracellular subunit stoichiometry of nicotinic receptors carrying mutations linked to autosomal dominant nocturnal frontal lobe epilepsy. Mol Pharmacol 75:1137-48.

Xu J, Cohen BN, Zhu Y, Dziewczapolski G, Panda S, Lester HA, Heinemann SF, and Contractor A (2011) Altered activity-rest patterns in mice with a human autosomal-dominant nocturnal frontal lobe epilepsy mutation in the beta2 nicotinic receptor. Mol Psychiatry 16:1048-61.

Zwart R, and Vijverberg HP (1998) Four pharmacologically distinct subtypes of a4b2 nicotinic acetylcholine receptor expressed in *Xenopus laevis* oocytes. Mol Pharmacol 54:1124-31.

# Chapter IV:
# Future Directions

To develop novel therapies for CNS disorders, we need to invest in our understanding of the basic biology and molecular details underlying neuronal processes. A systematic approach for the cholinergic system would be to attempt to characterize how ligands interact with their receptors at the biophysical level, which specific receptor subtypes they interact with, where those receptors are located subcellularly, on which neurons, how those neurons fit into larger circuits, and finally, how those circuits control behavior. Full characterization of these parameters will be challenging if not impossible in the near term due to experimental limitations. For example, we have limited tools to interrogate the expression levels of the two stoichiometries of α4β2. This thesis develops a novel method using SEP, which works in cell culture to corroborate the electrophysiological data, but may face challenges if attempted in vivo due to the presence of a wider variety of stochiometries including other subunits besides only α4 and β2.

If full characterization is intractable, we need to develop targeted hypotheses, test them rigorously across multiple laboratory models, and eventually test them in humans. To develop these hypotheses, however, systematic experiments should be used when they can generate a foundation for stronger hypothesis formulation. For example, one challenging aspect of studying lynx is that we know at least eight family members exist (lynx1-8), but we do not have good data on which lynx members bind to which nAChR subunits, and what the effect of binding may be on gating, desensitization, upregulation, or stoichiometry shifts. For some nAChR subunits that can be reliably expressed in heterologous expression systems, these experiments should be straightforward. For others, where expression is less reliable (i.e. α6), or harder to interpret (i.e. α5 incorporation into α4β2), it may be more difficult. While understanding the details of which lynx members bind to which nAChR

subtypes may not generate immediately exciting data, I expect these kinds of experiments to provide a solid foundation for further reaching hypotheses.

Armed with the knowledge of which lynx members bind specific nAChR subtypes, we could compare the overlap of expression of mRNA or protein across different types on neurons and in different locations and circuits. Single-cell mRNA quantification techniques exist, and could be used to possibly describe this overlap at the single cell level, which could lead to insights about which types actually interact in vivo. The next step would be to disrupt this interaction, which might be accomplished several ways, including using a small molecule or cell-permeable cyclic peptide to prevent the binding of lynx to the nAChR or subunit, knocking down lynx expression with anti-sense oligonucleotides (ASOs) or siRNA, increasing lynx expression via mRNA delivery, or using cell-impermeable proteins such as antibodies to disrupt lynx binding only at the plasma membrane without changing its intracellular effects.

Each of these methods will face unique challenges to implement. It is likely that advances in medicinal chemistry will be required for small molecule and cyclic peptide strategies, and advances in polymer science for ASO, siRNA, or mRNA drug delivery. Importantly, genetic knockout mice, which have already been made and characterized in several behavioral tests (Ibanez-Tallon et al., 2002; Miwa et al., 2006; Morishita et al., 2010), will continue to be a productive tool. Conditional knockouts will be important to retain the effects of lynx proteins through development, as there is evidence that it acts as a developmental switch, and to remove it from neural systems later as an initial proof of concept for pharmacological inhibition.

Optogenetics is a powerful technology that allows for precise localization and control over channel opening, which will lead to insights about circuit wiring and how to control behaviors at a molecular level. Although it will be challenging to implement in a patient, some are trying. More conventional methods may be more tractable in the short term, but an understanding of how circuits control behavior from optogenetics experiments will likely provide critical information to design those molecular therapies.

The specific work in this thesis on leads to multiple insights that deserve further experimental investigation. It has been clear for over a decade that two stoichiometries of α4β2 exist, and while there have been doubts as to whether both form in vivo, both stoichiometries are present in synaptosomes derived from brain tissue (Gotti et al., 2008). Several papers have shown that the β2VL mutation results in increased sensitivity of the receptor, and I show in this thesis that a shift in stoichiometry could be part of the molecular underpinning through both a shift in stoichiometry and greater incorporation of α5. It remains a mystery why the increased sensitivity, or selective loss of the low sensitivity component would lead to ADNFLE.

Based on the work in this thesis, the most plausible mechanism is that the β2VL mutation could drive greater incorporation of α5 into the α5α4β2 nAChRs, particularly in the cortex, where all necessary subunits are present and where ADNFLE seizures originate. Because α5-containing nAChRs have a higher permeability to calcium, and are thought to be responsible for increased long-range connectivity towards the outer layers of the cortex (Heath et al., 2010), the VL mutation could influence the development of α5-expressing neurons in the cortex, leading to hyperconnectivity and hypersynchrony, and ADNFLE. This hypothesis could be tested by crossing two existing mouse lines: the β2VL knock-in

with the α5 knockout mouse, and testing the crossed mice for both the behavioral abnormalities associated with b2VL mutation as well as taking brain sections to examine differences between the branching and length of neurons originating in the deep layers of the cortex. In the β2VL knockin/α5-KO mouse, I might also expect to find increased dendritic spines on those neurons. All of these hypotheses could be tested effectively by sectioning brain tissue and imaging via confocal microscopy. Finally, it would also be interesting to test the hypothesis that the α5 and β2VL containing nAChRs are more calcium permeable than α5α4β2-wt or α4β2-VL receptors. This would not only offer a plausible mechanism by which the mutation could cause ADNFLE, but also provide support for the hypothesis that increased intracellular calcium over the developmental period could lead to increased connectivity and chronic seizures.

Another line of experimentation that was not addressed here is the possibility that lynx1 could influence the sub-cellular localization of nAChRs. The GPI-anchor of lynx1 may interact with cholesterol rich lipid domains in the plasma membrane, thus controlling localization to synaptic, or perisynaptic regions by slowing diffusion through those regions. This hypothesis might be tested by labeling plasma membrane nAChRs with fluorescent particles that could be tracked at the single molecule level, such as quantum dots. I conducted several pilot experiments towards this goal, first labeling α7 with a quantum dot by first treating with biotinylatied α-bungarotoxin, then adding a streptavidin-conjugated quantum dot. I was able to label single α7 receptors, track them using custom tracking software, and calculate the mean square displacement (MSD) for each particle. Furthermore, removing cholesterol from the membrane with MB@@CD resulted in greater

diffusion as measured by MSD. This work was not pursued further in favor of the experiments in previous chapters.

I believe following up on these initial results could be promising, although challenges of adding or removing lynx1 remain. The initial pilot experiments were conducted on mouse day E16.5 cortical neurons isolated and re-plated in tissue culture dishes. The lynxKO mouse could serve as a source of lynx-free neurons as a control. However, there is uncertainty surrounding the expression of lynx1 by neurons from wild-type mice. We know that α7 is not expressed immediately upon plating cortical neurons; it takes 2-3 weeks to reach an expression level of α7 on the plasma membrane high enough to be detected by staining with α-bungarotoxin-AlexaFluor conjugates. Expression levels of lynx1 may be more variable from cell to cell, and will be more difficult to detect. As far as I know, currently there is now way to detect lynx1 via a fluorescent marker such as an AlexaFluor conjugate because there is no reliable source of specific antibody to lynx1 of which I am aware. Some antibodies may work for western blots, but there may not be enough sample from mouse cortical preparations to harvest enough protein. Even if enough protein were available, concerns about cell-to-cell variability in a tissue culture dish would make interpretation of plus/minus lynx experiments challenging in my opinion.

One solution is to make knock-in mice using the fluorescently tagged GFP-lynx1, mCherry-lynx1, and SEP-lynx1 constructs that I developed. Using these tools, we could harvest the same mouse cortical neurons and know which cells are expressing lynx1 in culture, and even in vivo by taking brain slices and performing confocal imaging experiments. Before investing the time and resources to create knock-in mice, it may be advisable to conduct a more thorough comparison of the fluorescently tagged lynx1

variants to wild-type lynx1. Although I saw very similar results with the two types of lynx1, in my opinion, the magnitude of the investment in a knock-in mouse warrants additional characterization across multiple models.

Alternatively, as I have shown that lynx1 interacts with the α4 nAChR subunit in the ER, the GPI-anchor could be important in segregating either individual subunits or fully assembled pentamers to specific regions of the ER for export to the plasma membrane, export to specific compartments of the plasma membrane, or possibly retention in the ER. GPI-anchored proteins have been reported to be directly targeted to the apical domain of cells (Paladino et al., 2006), or the axons of neurons. To my knowledge, this thesis contains the first data to demonstrate the binding of a GPI-anchored protein to influence the assembly of a multi-subunit complex in the ER. The possibility that a GPI-anchored protein may also exert influence by regulating the trafficking of its binding partners would be both novel and highly interesting.

Pharmacological manipulation of lynx1 provides a novel and interesting way to indirectly target nAChRs, potentially gaining greater specificity than direct modulation of the receptor. Many more experiments are necessary to understand the molecular interactions and the biological importance of interactions between lynx family members and nAChRs. Both systematic, exploratory, hypothesis-generating experiments, in addition to targeted and rigorous experiments designed to test hypothesis of high biological importance should be conducted to move the field forward. A greater understanding the biology of nAChRs is likely to lead to critical insights about neuroscience and better treatments for a wide range of CNS disorders including addiction, and cognitive and psychiatric disorders.

# References

Gotti, C., Moretti, M., Meinerz, N., Clementi, F., Gaimarri, A., Collins, A.C., and Marks, M.J. (2008). Partial deletion of the nicotinic cholinergic receptor α4 and β2 subunit genes changes the acetylcholine sensitivity of receptor mediated $^{86}Rb^{+}$ efflux in cortex and thalamus and alters relative expression of α4 and β2 subunits. Mol Pharmacol.

Heath, C.J., King, S.L., Gotti, C., Marks, M.J., and Picciotto, M.R. (2010). Cortico-thalamic connectivity is vulnerable to nicotine exposure during early postnatal development through α4/β2/α5 nicotinic acetylcholine receptors. Neuropsychopharmacology *35*, 2324-2338.

Ibanez-Tallon, I., Miwa, J.M., Wang, H.L., Adams, N.C., Crabtree, G.W., Sine, S.M., and Heintz, N. (2002). Novel modulation of neuronal nicotinic acetylcholine receptors by association with the endogenous prototoxin lynx1. Neuron *33*, 893-903.

Miwa, J.M., Stevens, T.R., King, S.L., Caldarone, B.J., Ibanez-Tallon, I., Xiao, C., Fitzsimonds, R.M., Pavlides, C., Lester, H.A., Picciotto, M.R.*, et al.* (2006). The Prototoxin lynx1 Acts on Nicotinic Acetylcholine Receptors to Balance Neuronal Activity and Survival In Vivo. Neuron *51*, 587-600.

Morishita, H., Miwa, J., Heintz, N., and Hensch, T. (2010). Lynx1, a cholinergic brake, limits plasticity in adult visual cortex. Science *330*, 1238-1240.

Paladino, S., Pocard, T., Catino, M.A., and Zurzolo, C. (2006). GPI-anchored proteins are directly targeted to the apical surface in fully polarized MDCK cells. The Journal of cell biology *172*, 1023-1034.